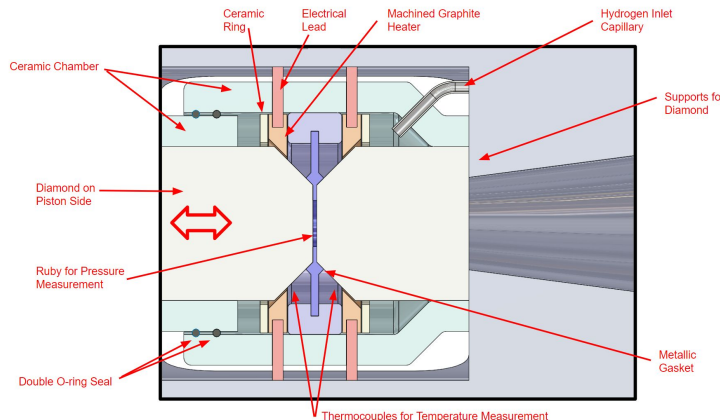


Diamond Anvil Measurement of Muon Catalyzed D-D Fusion Kinetics

The dMu/DT Collaboration



J.A. Allen, R. Chaney, D.M. Harrington, P.A. Holden^a, J.T. Hinchin, [A.N. Knaian](#),
E. Koukina, [K.R. Lynch](#), N.A. MacFadden, S.O. Newburg, K. Payne, I.D. Spool

Open CHRISP Users Meeting BV52, 27 January 2021
[A.N. Knaian](#), [NK Labs, LLC](#), Cambridge, Massachusetts, USA
[K.R. Lynch](#), [York College](#), Jamaica, New York, USA

BETHE program



Image: US Department of Energy

Program Description:

Breakthroughs Enabling Thermonuclear-fusion Energy (BETHE) supports the development of timely, commercially viable fusion energy. Building on recent progress in fusion research and synergies with the **growing private fusion industry**, this program aims to deliver a larger number of higher maturity, lower cost fusion options via three research categories: (1) **Concept Development to advance the performance of inherently lower cost but less mature fusion concepts**; (2) Component Technology Development that could significantly reduce the capital cost of higher cost, more mature fusion concepts; and (3) Capability Teams to improve/adapt and apply existing capabilities (e.g., theory/modeling, machine learning, or engineering design/fabrication) to accelerate the development of multiple concepts. BETHE's technology-to-market component aims to build and smooth the path to fusion commercialization to include public, private, and philanthropic partnerships.



Ara Knaian
Principal Investigator



Kevin Lynch
Co-Principal
Investigator



Seth Newburg, Chemistry



Joe Allen
FPGA Development



Rachel Chaney
Electrical Design



Demetrious Harrington
Optical Design



JT Hinch
High Pressure Cell



Pat Holden
Software



Elena Koukina
Simulation



Karl Payne
Simulation



Ira Spool
Mechanical Design

Goals of the project

- Measure key rate and efficiency parameters at higher temperatures and pressures than have been explored previously

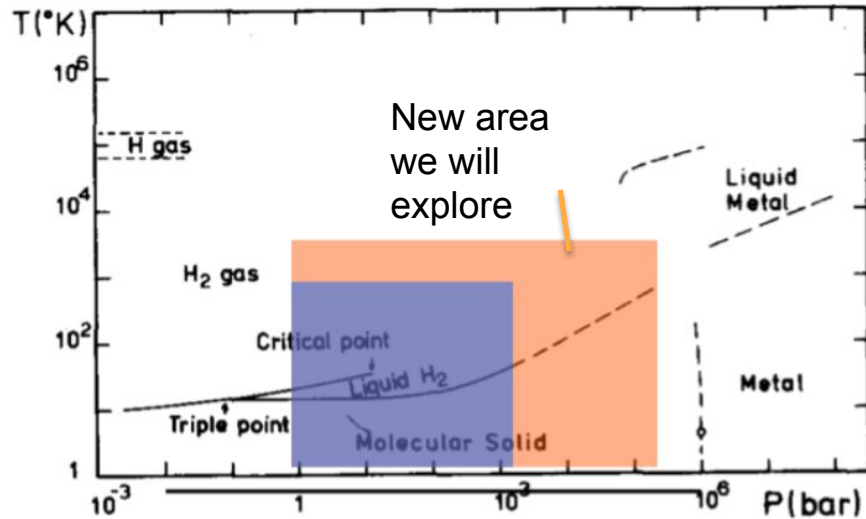


Diagram from Leung, W. B., March, N. H., & Motz, H. (1976). Primitive phase diagram for hydrogen. Physics Letters A, 56(6), 425–426.

- Create high-fidelity physics process models for GEANT4, to enable reactor design innovation

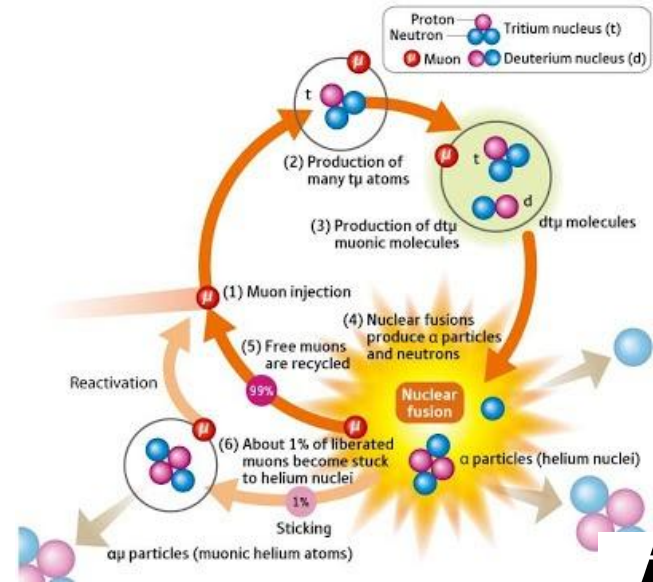


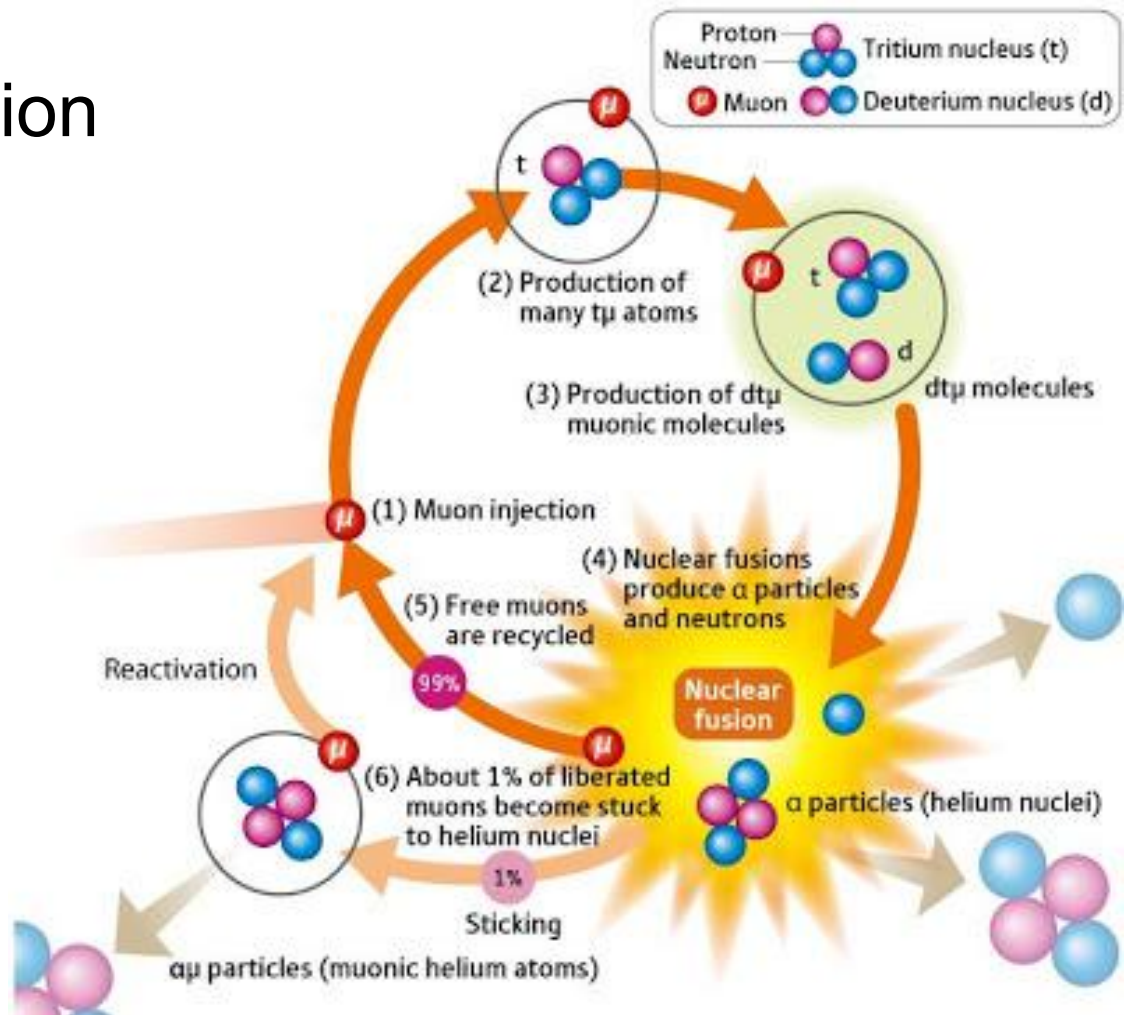
Figure: B. Wang, 2009

Physics motivation

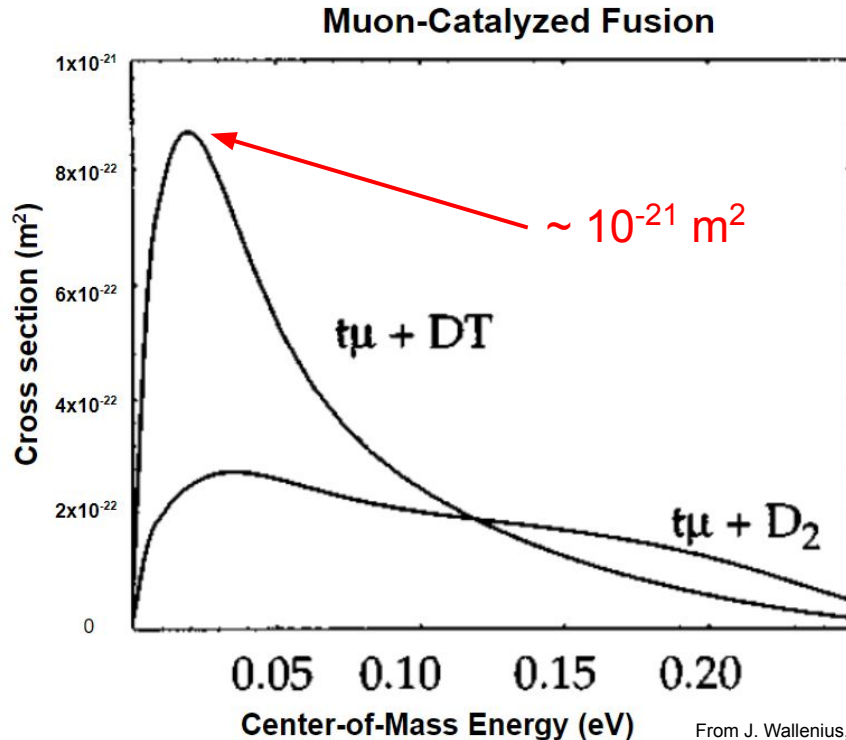
Muon-catalyzed fusion

Key physical parameters:

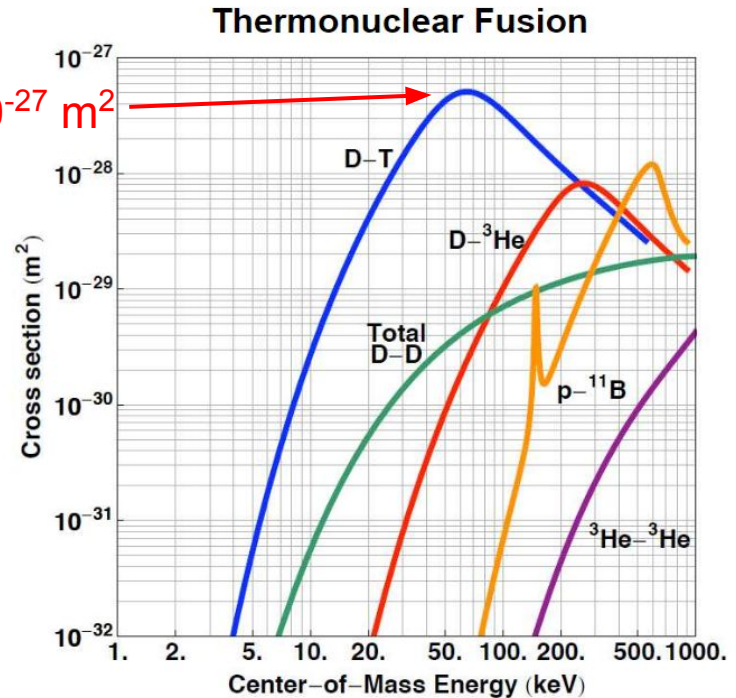
- Cycling rate - fusions per second
- Sticking fraction - fraction of muons carried off by alphas



muCF is interesting because of large cross section



From J. Wallenius, P. Froelich,
Formation of metastable dtmu
molecules in $t\mu(2s)$ -D2 collisions,
Physical Review A, Vol 54, No. 2, 1996



From Wikimedia
Commons

Temperature and density increase cycling rate

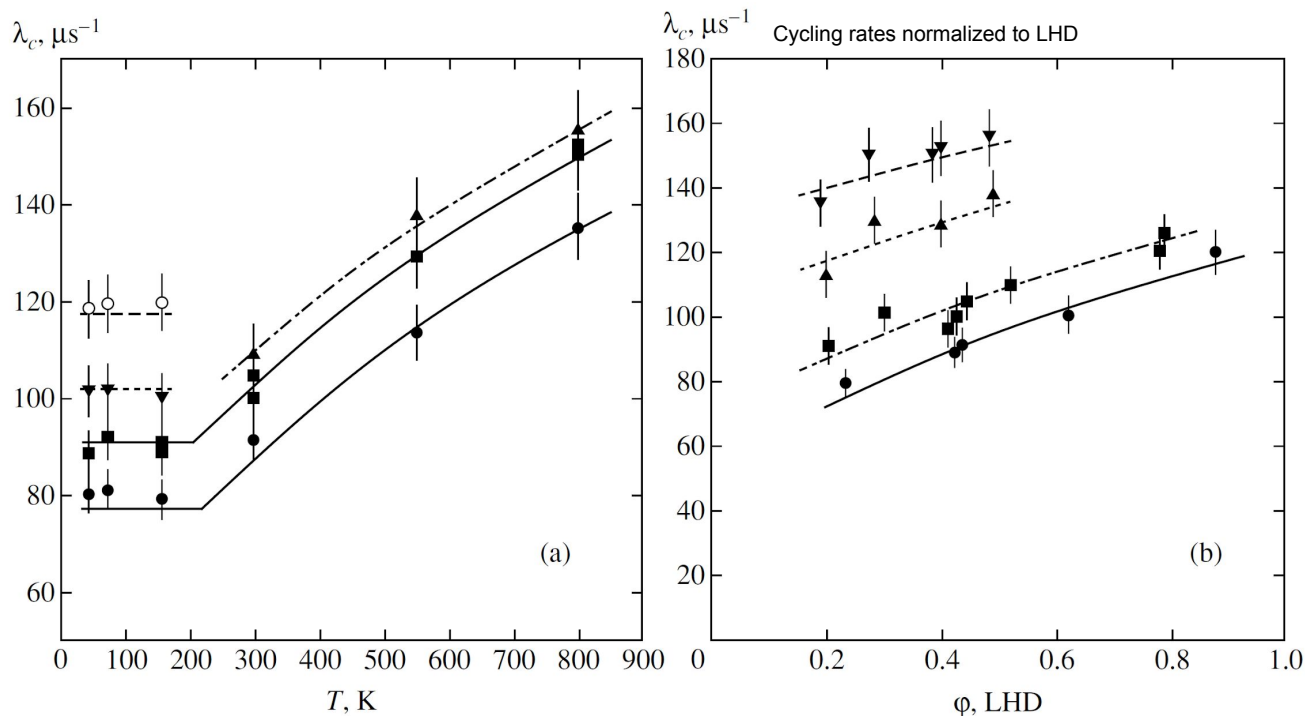
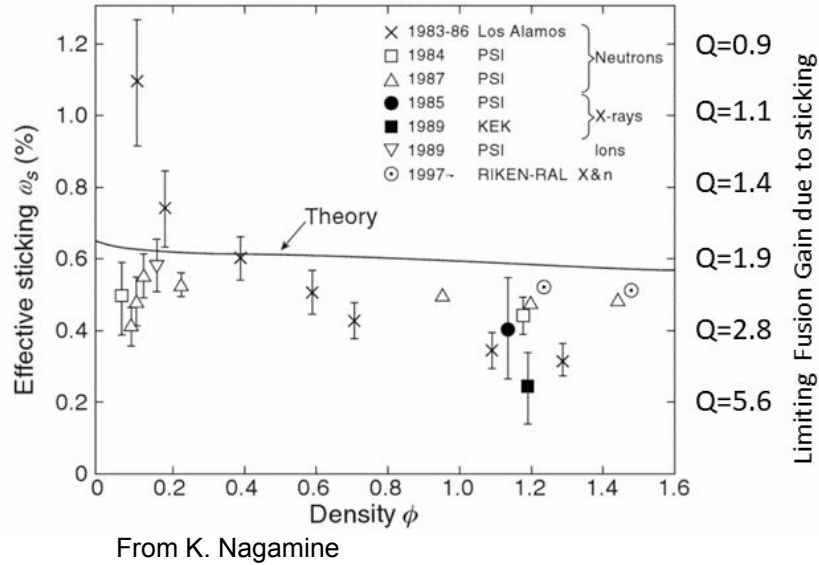


Fig. 12. (a) Normalized cycling rates as a function of temperature for the gaseous D/T mixture at $C_T \approx 33\%$ and different densities $\phi = 0.88-0.91$ (\circ), $0.62-0.64$ (\blacktriangledown), $0.49-0.52$ (\blacktriangle), $0.39-0.45$ (\blacksquare), $0.19-0.24$ (\bullet) LHD. (b) Normalized cycling rates as a function of density for the gaseous D/T mixture at $C_T \approx 33\%$ and different temperatures $T = 800$ K, $C_T = 0.34-0.36$ (\blacktriangledown); $T = 550$ K, $C_T = 0.33-0.36$ (\blacktriangle); $T = 300$ K, $C_T = 0.31-0.36$ (\blacksquare); $T = 158$ K, $C_T = 0.31$ (\bullet). The curves are obtained with optimum parameters.

Do these trends continue to higher temperature and density?

(From Bom, et. al, "Experimental Investigation of Muon-Catalyzed D-T Fusion in Wide Ranges of D-T Mixture Conditions", Journal of Experimental and Theoretical Physics, Vol 100, No. 4, 2005)

Sticking (and fusion gain!) versus density



Data lies below theoretical expectations, and tantalizingly close to the commercially interesting value of $Q=5$... how does this extend to higher density systems?

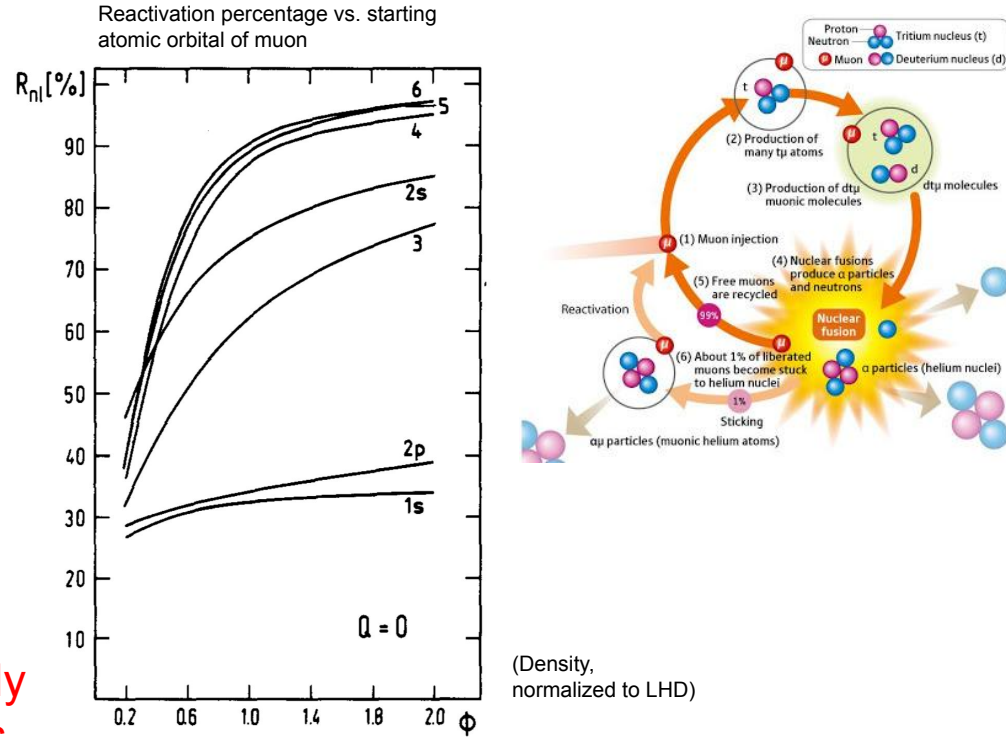


Fig. 2: Reactivation probabilities R_{nl} no 2p-2s quenching, (b) $Q=1$: From H. Rafelski, Muon Reactivation in Muon-Catalyzed D-T Fusion

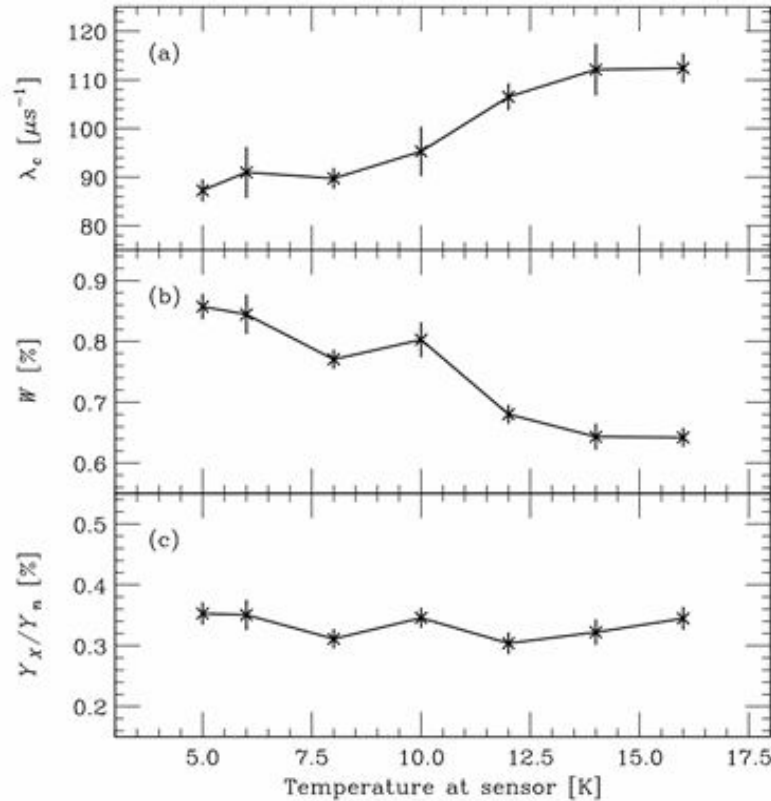
Temperature dependence of sticking???

(Kawamura / Nagamine)

Cycling rate

Sticking fraction

X-ray to neutron
yield ratio

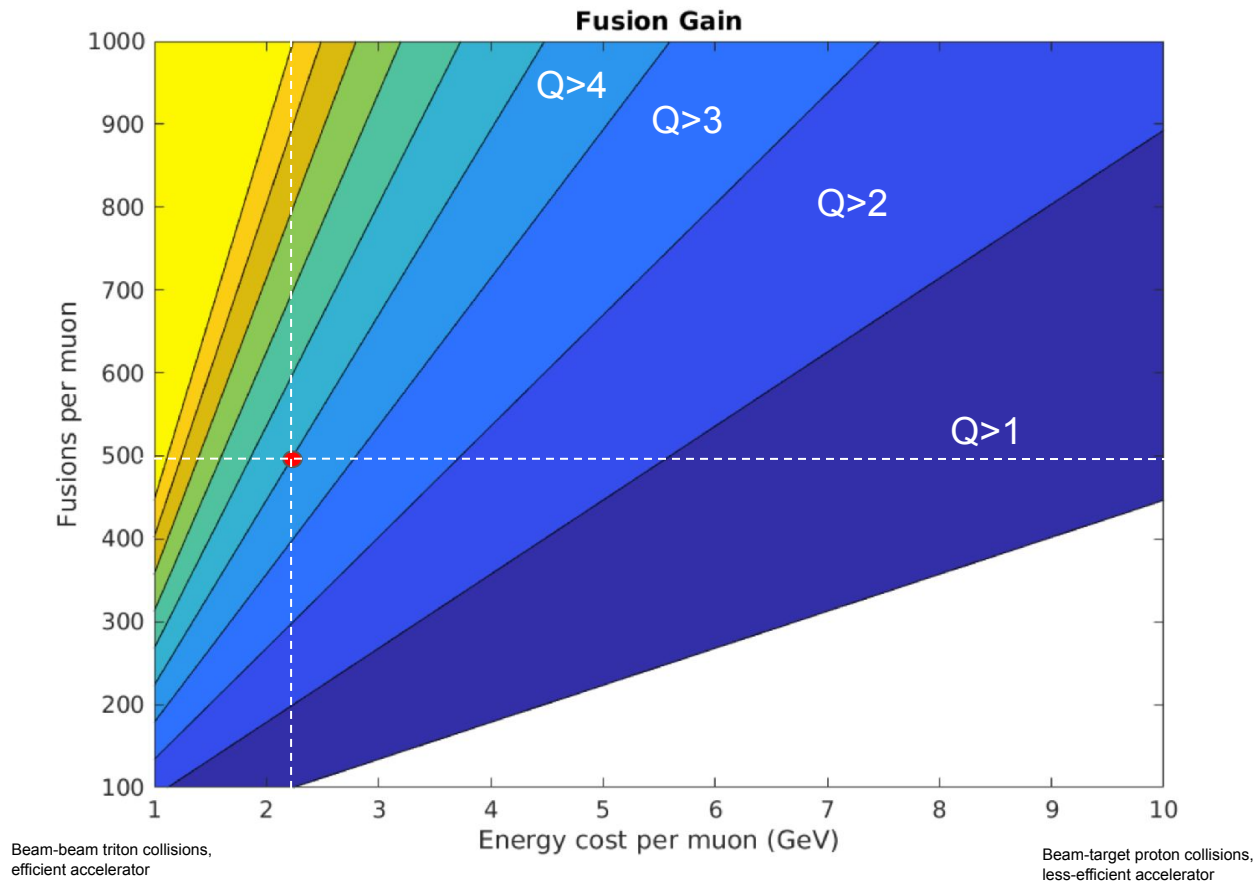


The observed temperature dependence of sticking at low T is unexpected ... this suggests details of the sticking and reactivation physics are not well understood

Figure R2: Observed anomalous dependence of effective sticking percentage (W) on temperature. Figure from [Kawamura10]

Technology motivation

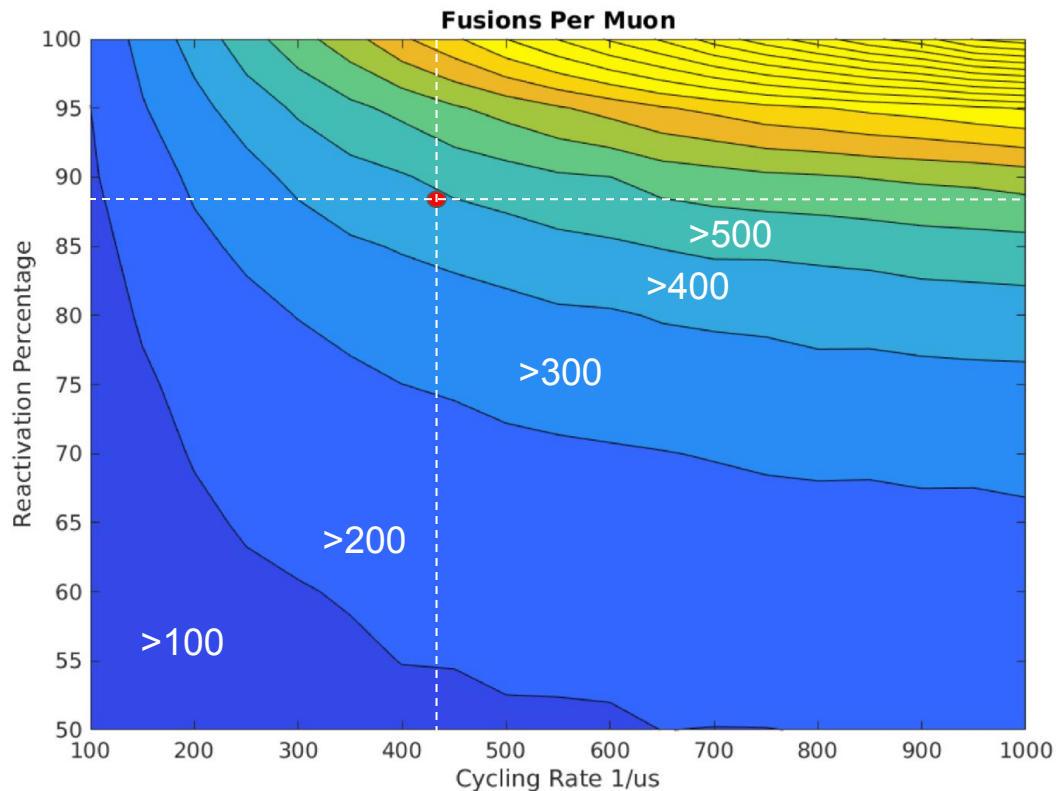
Design charts: Fusion gain



$$Q = 22.4\text{MeV} \times \frac{N_{fusions/\mu}}{E_{\mu}}$$

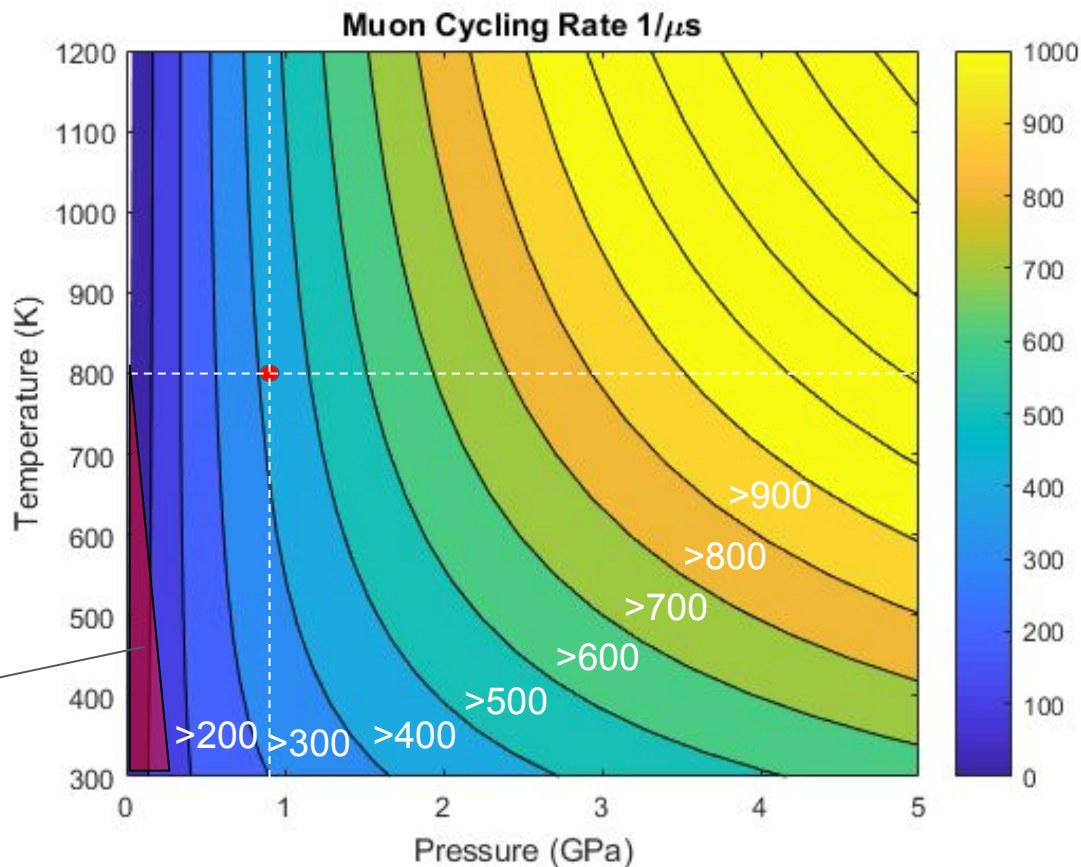
Includes heat from tritium breeding. (after R. Kelly)

Design charts: Fusions per muon



From Monte Carlo simulation of the Markov chain, taking into account the muon lifetime and initial sticking of 0.88%

Design charts: Muon cycling rate estimate



From bilinear fit of Los Alamos gas-phase muon cycling rate data and the NIST equation of state for deuterium. Caution: This figure is an extrapolation for $T > 600$ K and density above 0.7 LHD.

Doing this measurement will allow making an accurate version of this chart.

Path to efficient muon production

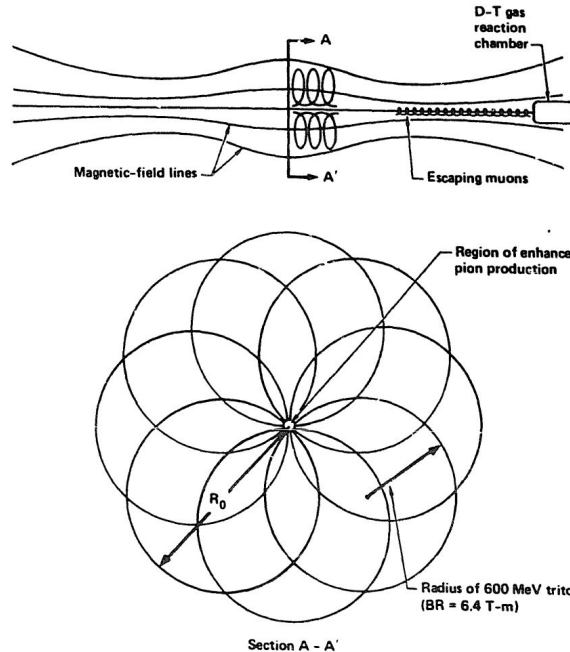


Fig. 1. Arrangement of triton orbits leading to enhanced muon production near the axis.

Chapline, G. F., & Moir, R. W. (1988). Production of muons for fusion catalysis using a migma configuration. Nuclear Instruments and Methods in Physics Research Section A: Accelerators, Spectrometers, Detectors and Associated Equipment, 271(1), 203–206.

Path to reactivation enhancement

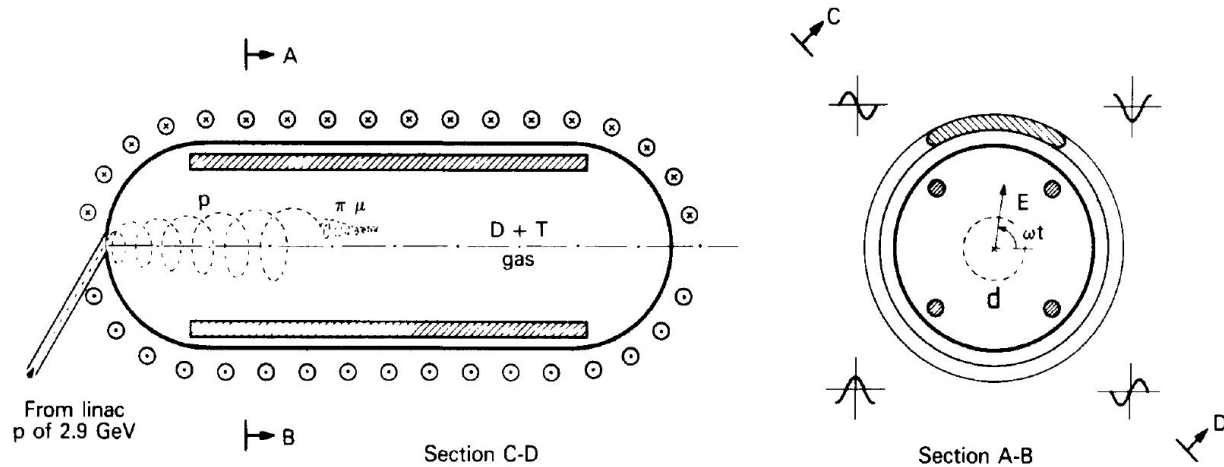
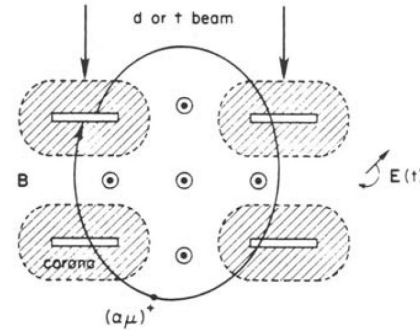
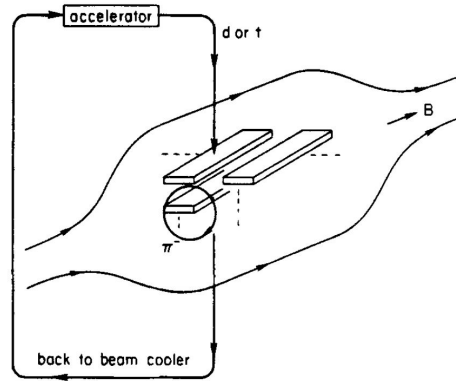


Fig. 1. Sketch of the proposed μ CF reactor. The reaction volume confined by a vessel is filled with a D-T gas mixture at high temperature. A coil forms a magnetic bottle of high field strength. The rotating electric field E is produced by four electrodes, indicated by hatching from lower left to upper right, at radio-frequency voltages with a 90-deg phase shift between neighboring electrodes.

H. Daniel, "Concept of a Novel Muon-Catalyzed Fusion Reactor",
Fusion Technology, Volume 20, Issue 2, 1991

Path to high rate AND high reactivation



T. Tajima, S. Eliezer, R.M. Kulsrud, "A new concept for a muon catalyzed Fusion Reactor", AIP Conference Proceedings, 181, 423, 1988



Separation of scales

- At LHD, particle energies and ranges for D-T:
 - 3 keV muon: ~ 0.001 mm
 - 10 eV hot muonic atom: ~ 0.001 mm
 - 3.5 MeV alpha: ~ 0.1 mm
 - 3.5 MeV muonic alpha: ~ 1 mm
- If there is a thin layer, filament, or droplet of fuel, when a muon stops there, the next N fusions will happen near the same spot.

Microencapsulated fuel

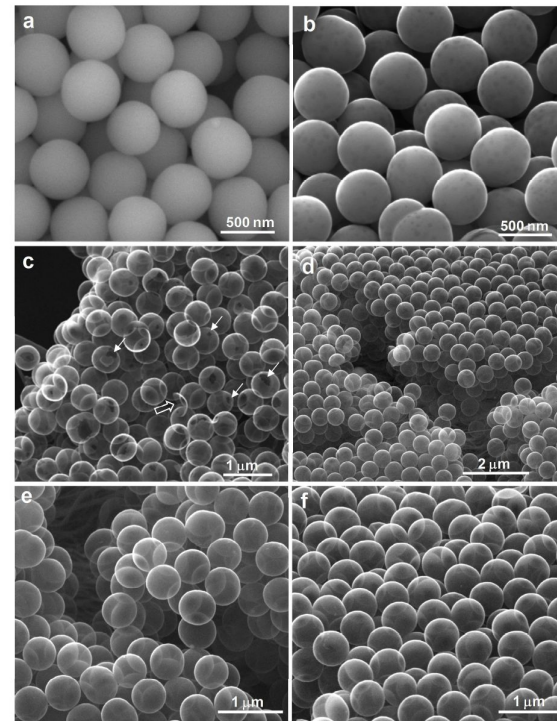
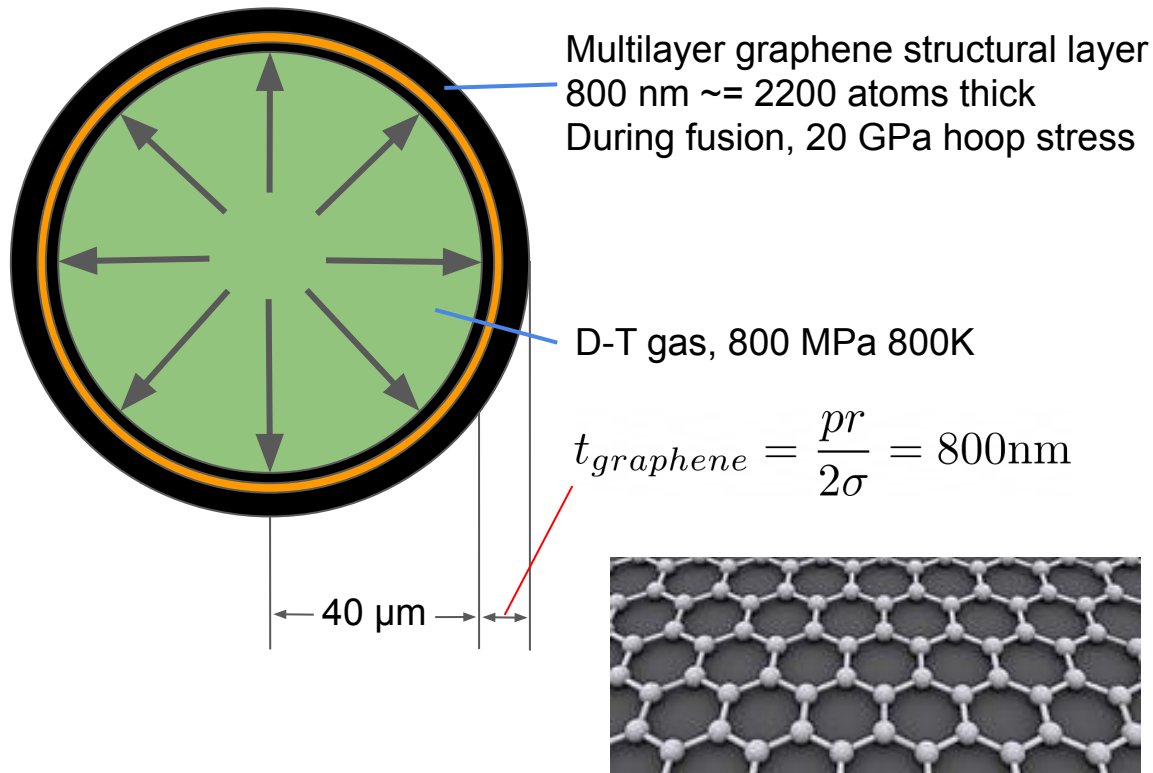


Figure from X. Li, M. Chi, S.M. Mahurin, R. Liu, Y.-J. Chuang, S. Dai, Z. Pan, Graphitized hollow carbon spheres and yolk-structured carbon spheres fabricated by metal-catalyst-free chemical vapor deposition, Carbon (2016)

The World's Smallest Gas Cylinders?

G. E. Gadd,* M. Blackford, S. Moricca, N. Webb, P. J. Evans,
A. M. Smith, G. Jacobsen, S. Leung, A. Day, Q. Hua

Argon gas was trapped at high pressure within hollow carbon tubes grown in vapor that have an outer diameter of between 20 and 150 nanometers. The gas was forced into the tubes by hot isostatically pressing (HIPing) the carbon material for 48 hours at 650°C under an argon pressure of 170 megapascals. Energy dispersive x-ray spectroscopy maps and line scans across the tubes show that the argon is trapped inside the bore and not in the tube walls. The room temperature argon pressure in these tubes was estimated to be about 60 megapascals, which indicates that equilibrium pressure was attained within the tubes at the HIPing temperature. These findings demonstrate the potential for storing gases in such carbon structures.

of the tube. In several of these tubes, the Ar content was very high, and, furthermore, it appeared to be contained in the cavity of these tubes (Fig. 2).

An x-ray map of an Ar-filled tube (Fig.

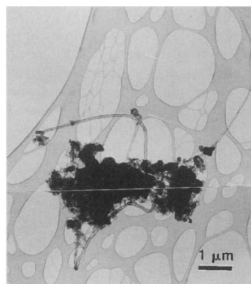


Fig. 1. A montage of two TEM images that shows two hollow carbon tubes intertwined in dense metallic-based material. The tube on the left was found to contain Ar at high pressure, whereas the tube on the upper right was empty. A montage was needed because the overall length of the tubes was too large for a single image.

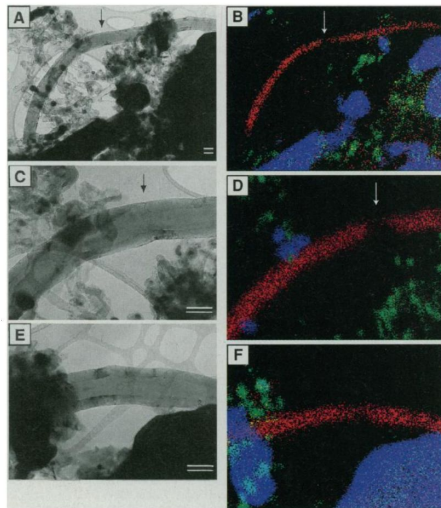


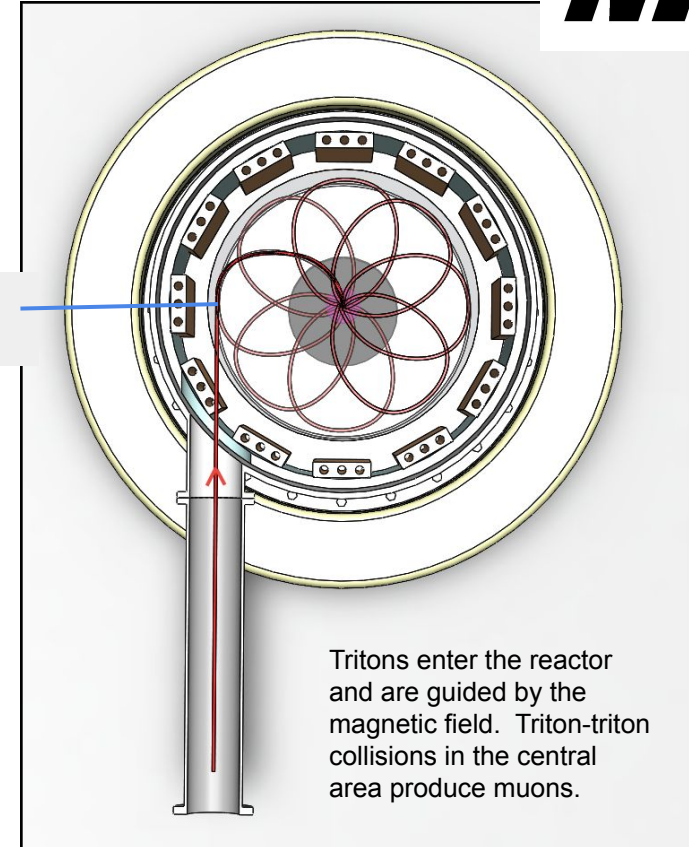
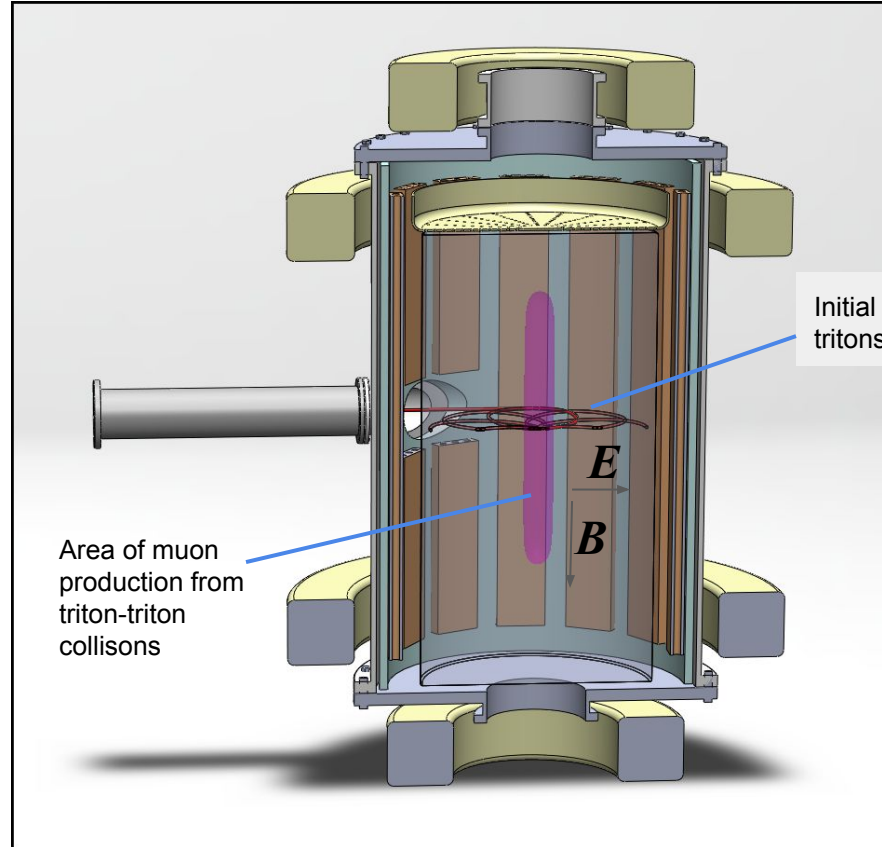
Fig. 2. TEM images and x-ray maps of a typical Ar-filled tube that winds its way through dense solid material. The C tube is clearly seen to be hollow and has an outer diameter of 140 nm and an inner bore diameter of 60 nm. (A), (C), and (E) show TEM images, whereas (B), (D), and (F) display the corresponding x-ray map images. In the latter panels, the K α x-ray emissions from Ar, Fe, and Zn are shown in red, green, and blue, respectively. A discontinuity in the tube is indicated in the images by the arrows. The scale bars on (A), (C), and (E) represent 100 nm.

60 MPa gas pressure Argon was stored
a single-atom-thick carbon nanotube

$$\frac{60\text{MPa} \times 150\text{nm}}{2 \times 0.617\text{\AA}} = 73\text{GPa}$$

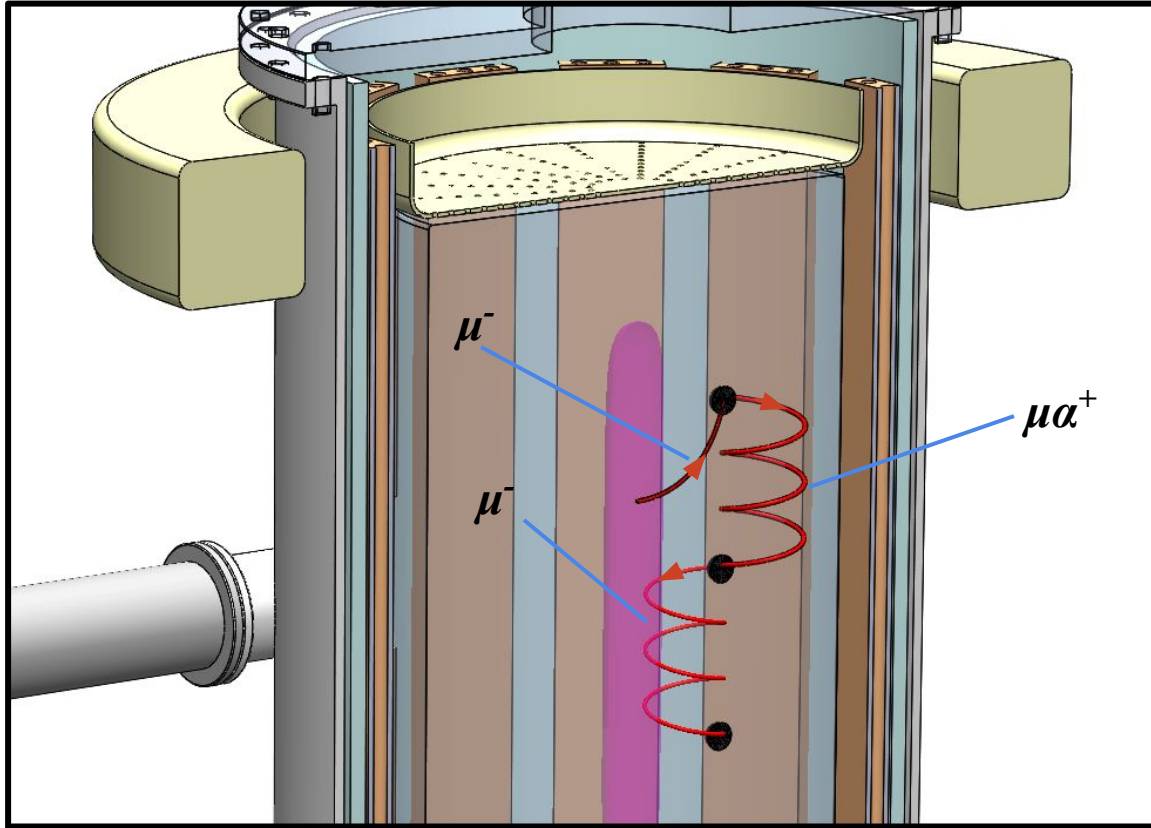
Equivalent to 73 GPa hoop stress!

Reactor sketch: Internal muon production



3m overall dia @ 10T

Reactor sketch: Enhanced reactivation



Fuel microcapsules are shown enlarged for clarity. Muonic alpha particles (from sticking) are confined by the magnetic field accelerated by the rotating electric field until the muon is ionized by collisions.

Proposed Experiment for First Beam Period

Diamond anvil cell

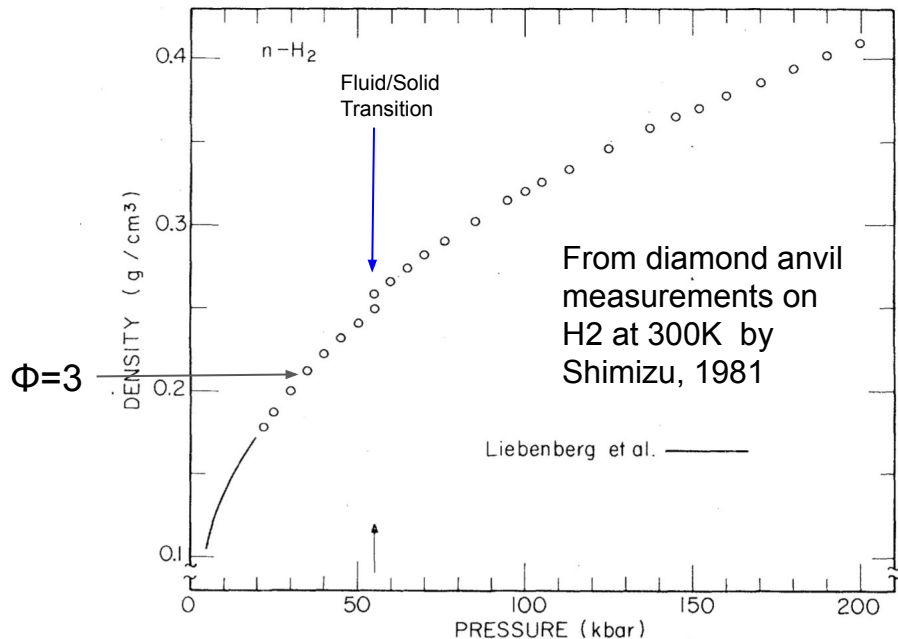
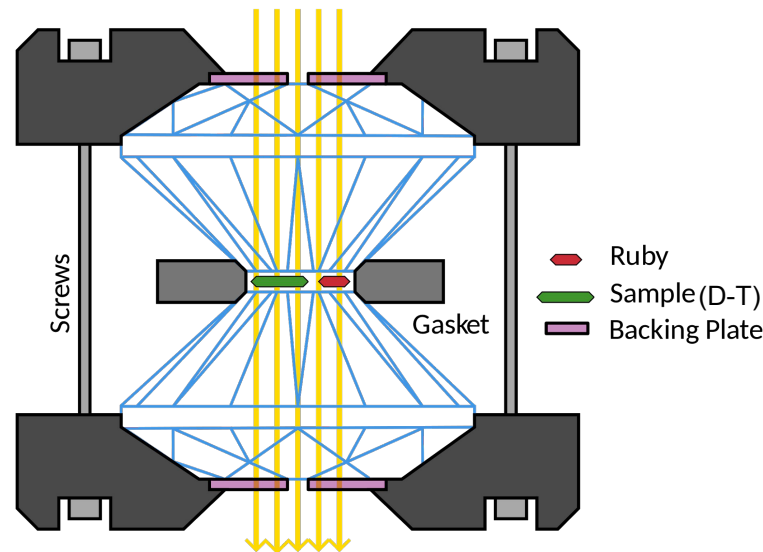


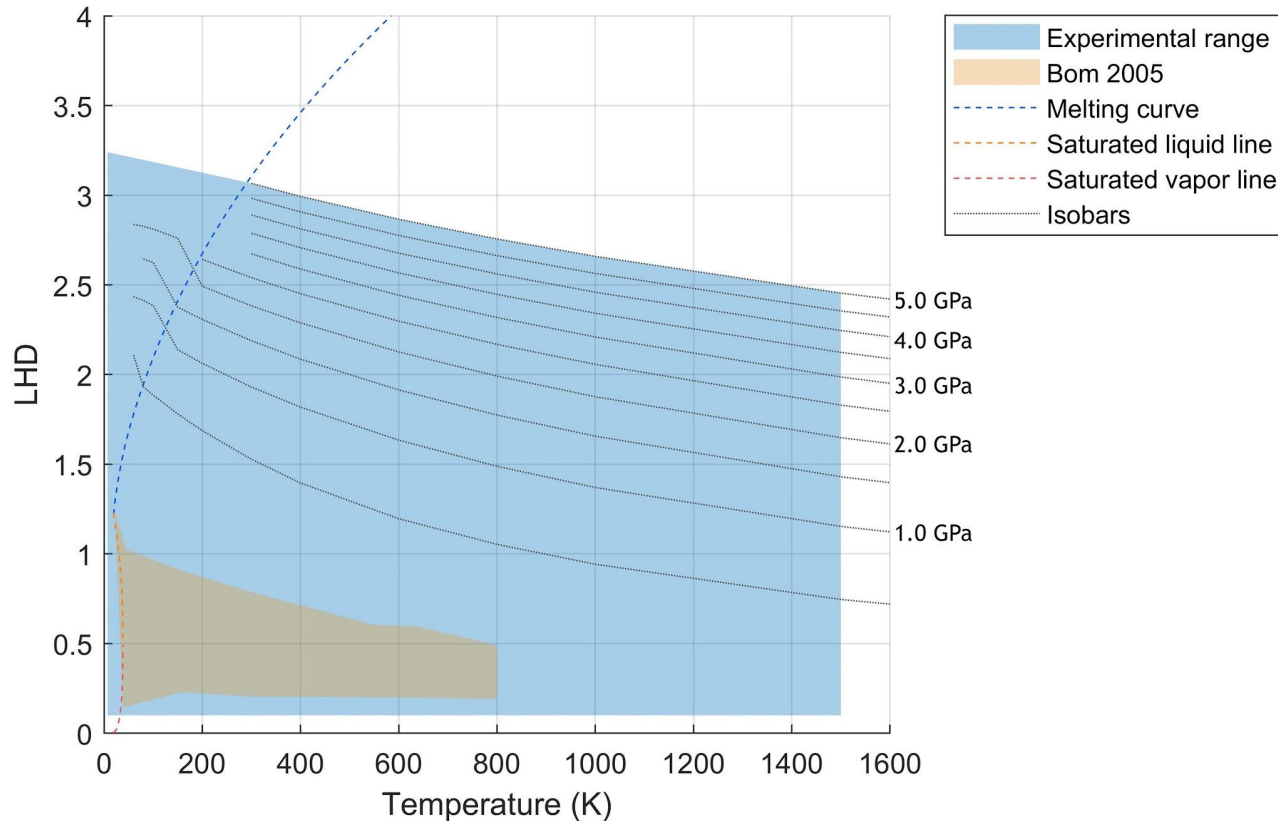
FIG. 4. Density of $n\text{-H}_2$ as a function of pressure. Open circles show the present result and solid line shows the result by Liebenberg *et al.* (Ref. 4).

Shimizu, E. M. Brody, H. K. Mao, and P. M. Bell, Phys. Rev. Lett. 47, 128 (1981).

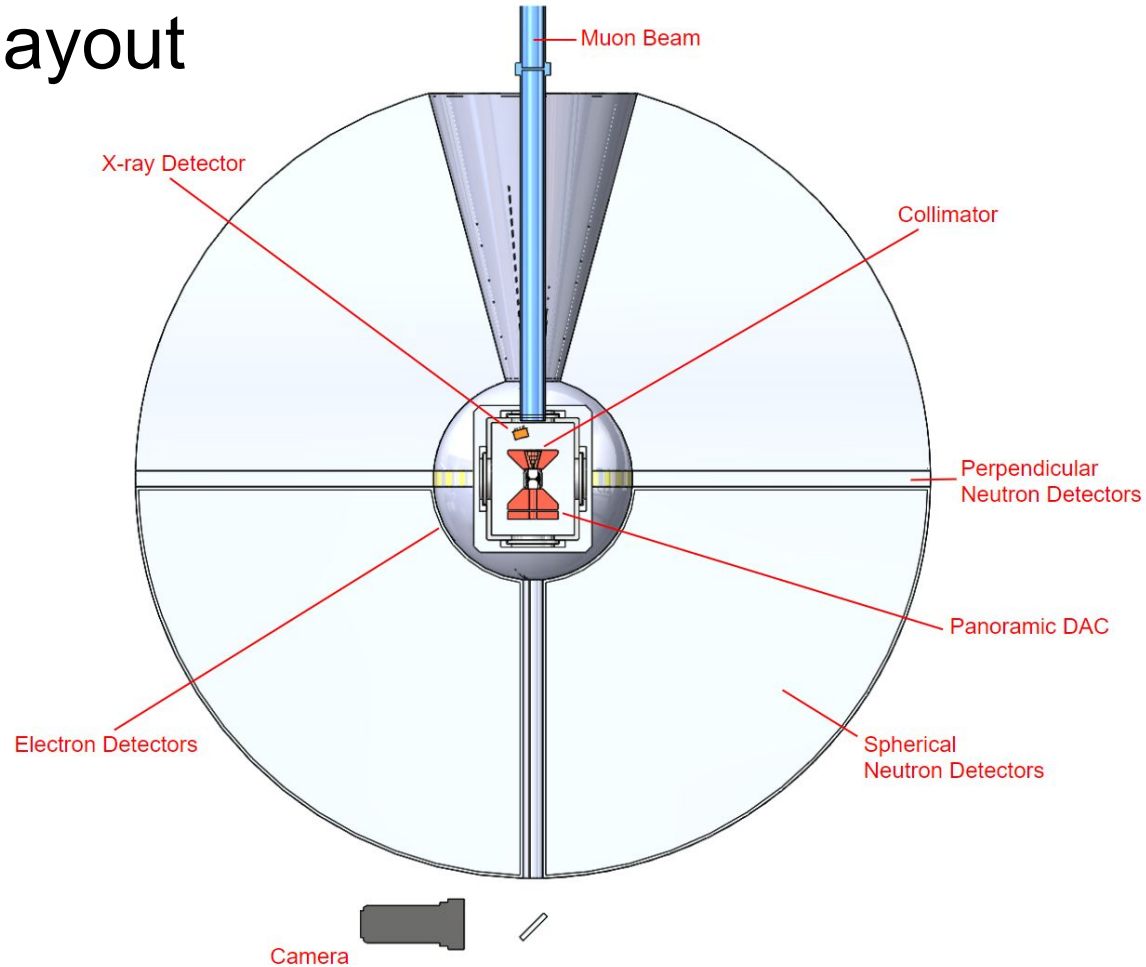


Diamond anvil cell can be used to achieve up to 770 GPa / 7000 K. We need only 5 GPa / 1500 K.

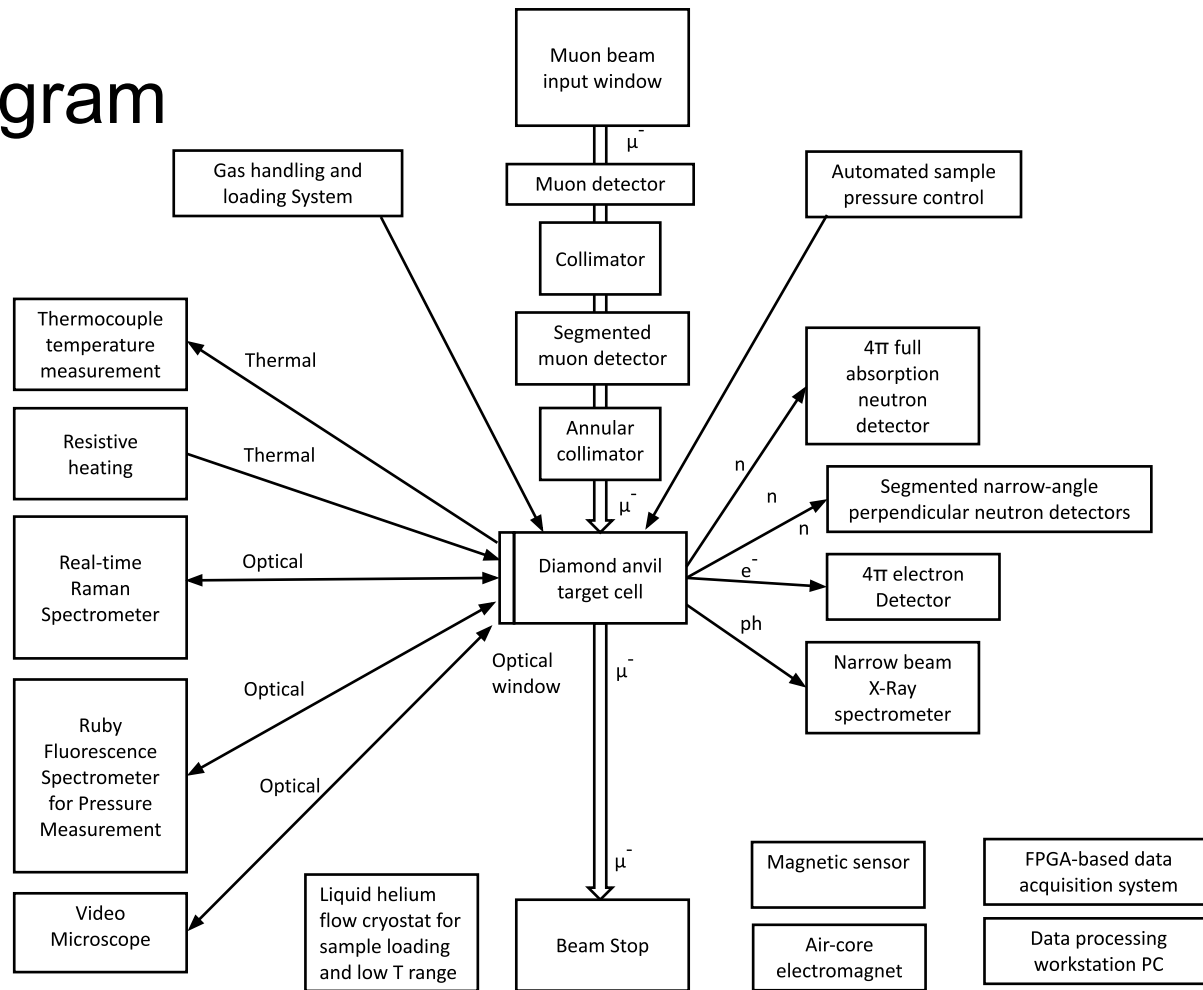
Temperature and pressure range



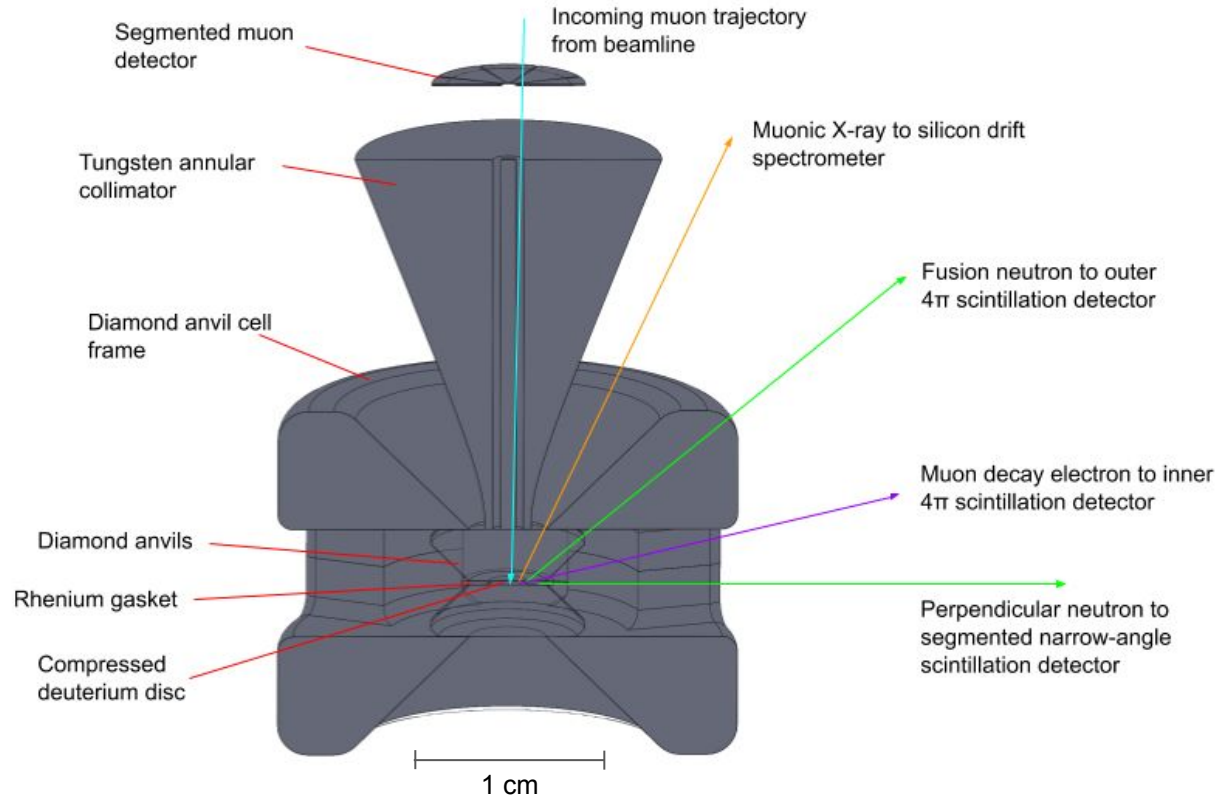
Detector layout



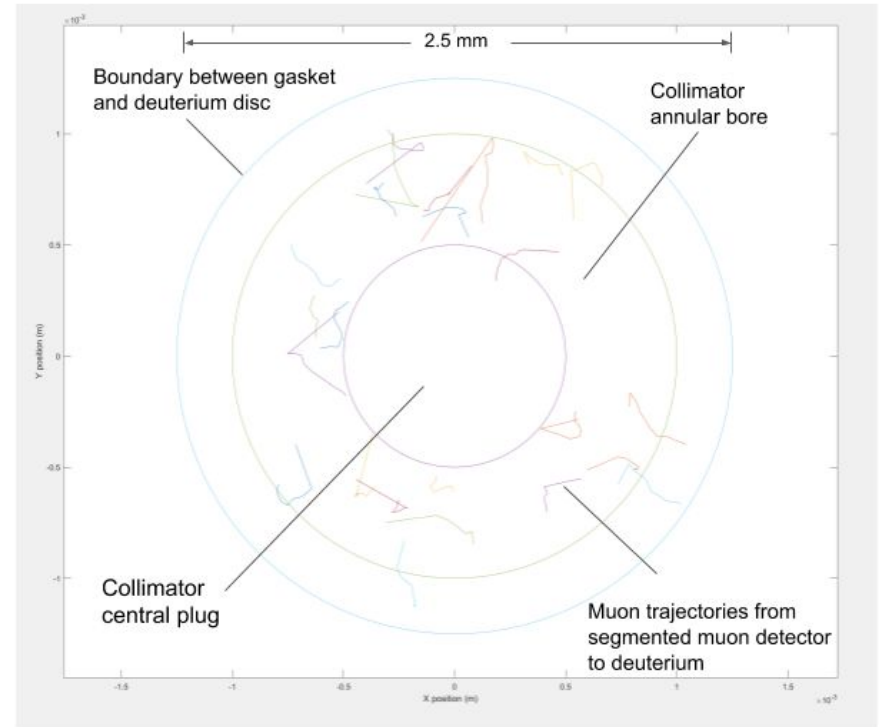
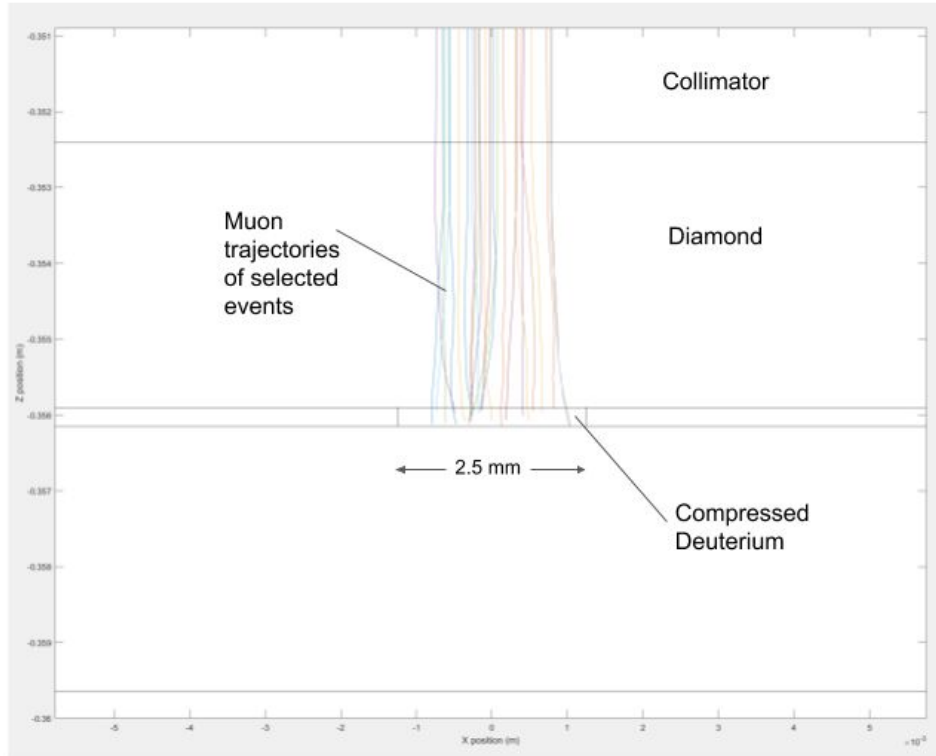
Block diagram



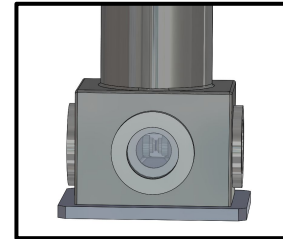
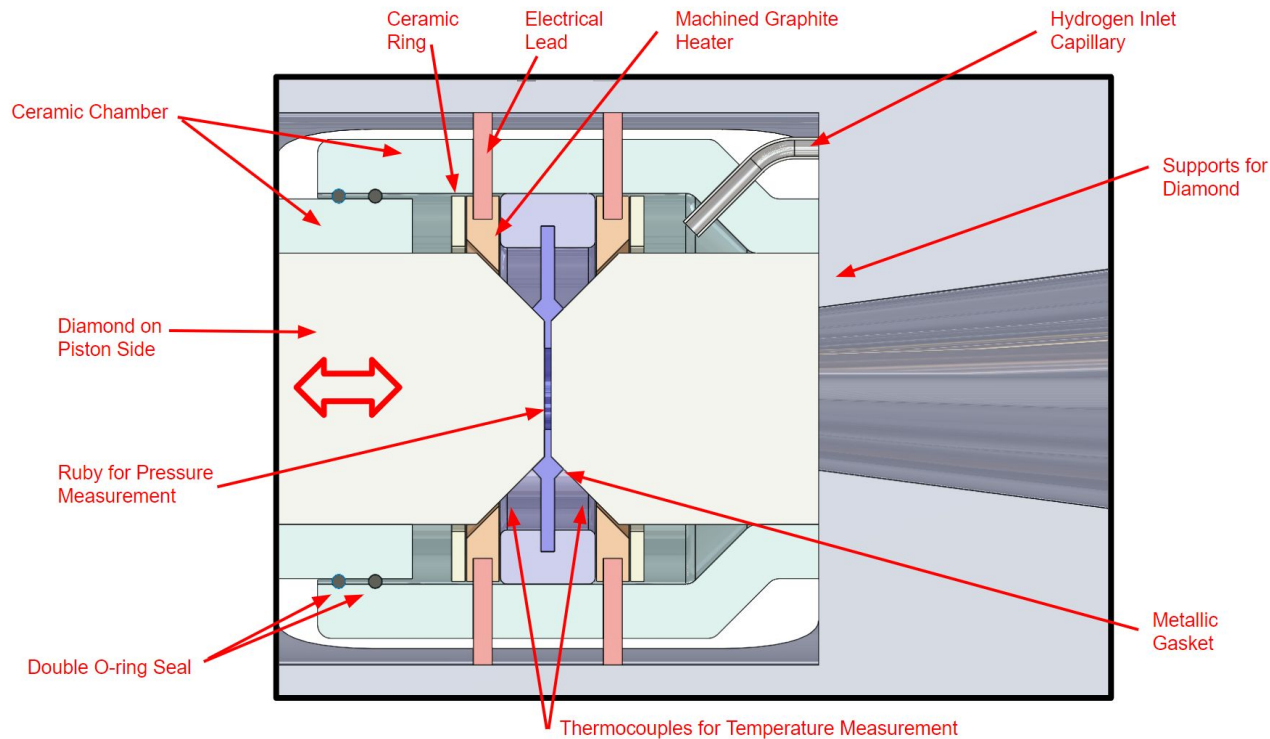
Muon detector, collimator, and target cell



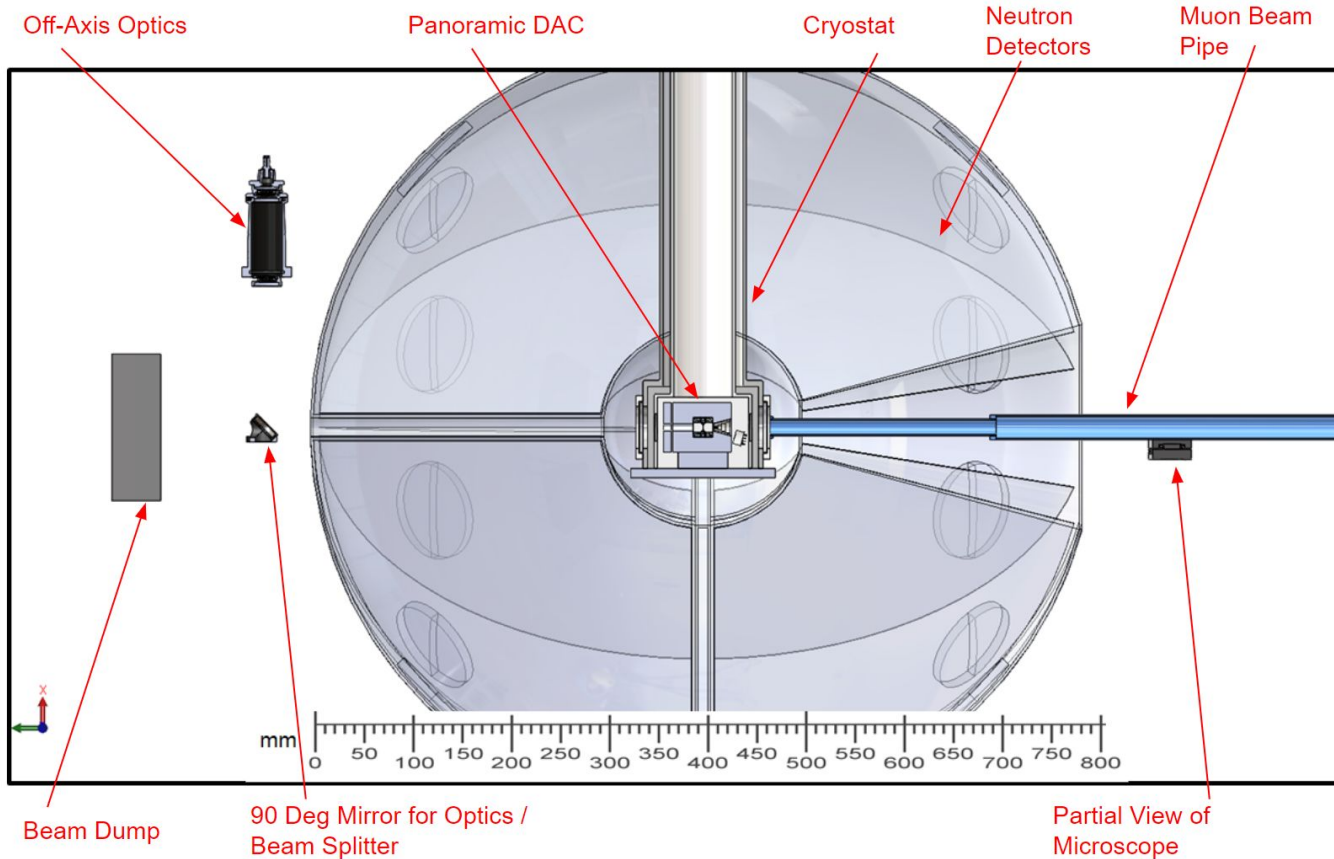
GEANT4 trajectories of primary (μ^-) from events passing selection criteria



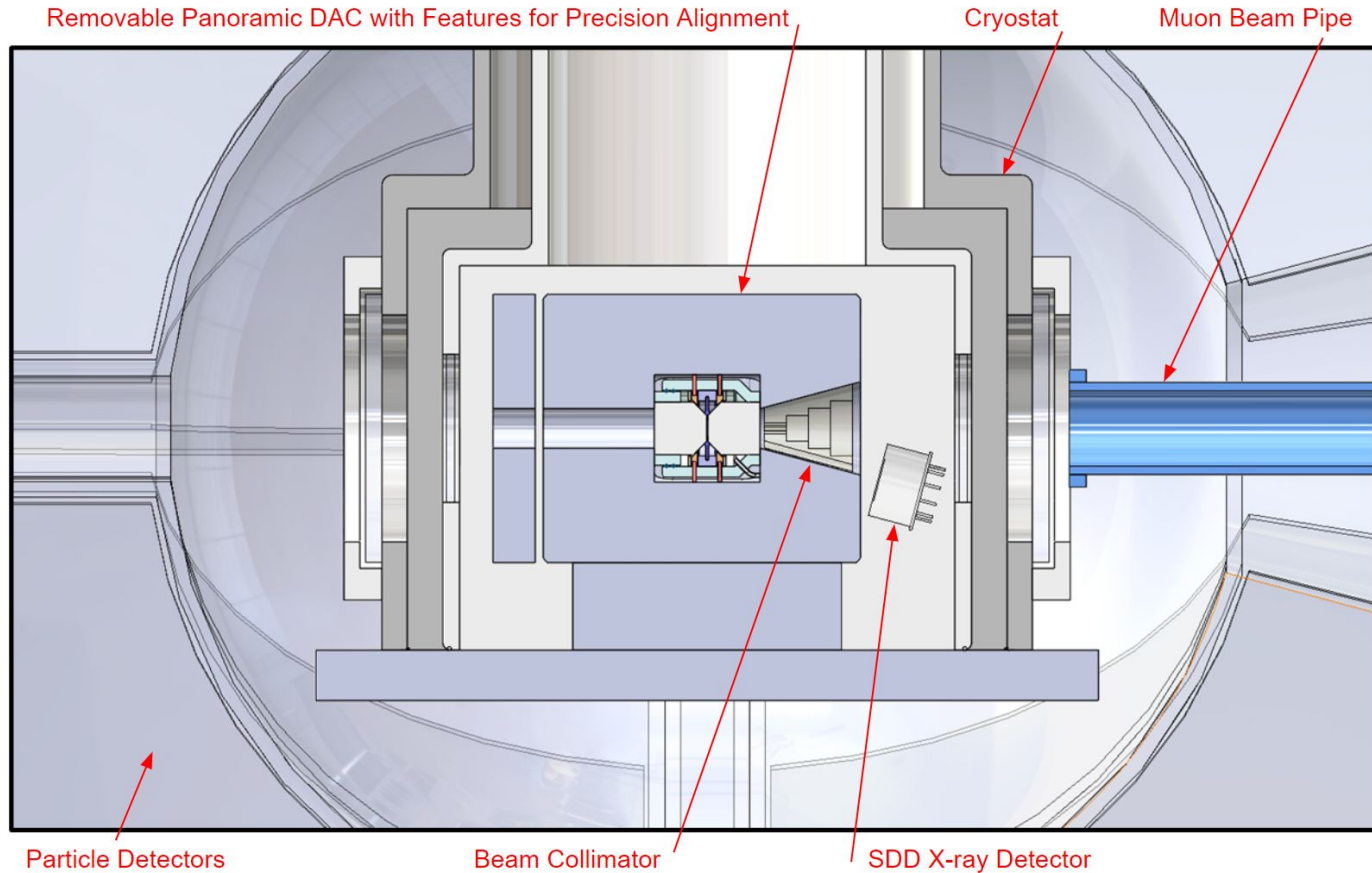
Sample loading, compression and heating



Cryostat integration with detectors



X-ray spectrometer inside cryostat



End-to-end simulations with GEANT4

Geant4 version Name: geant4-10-00

<< in Multi-threaded mode >>

Copyright

References

Number of threads is forced to

Read /physics/useOpticalPhysics %

<<< Geant4 Physics List simulation

Visualization Manager instantiating

Visualization Manager initialising

Registering graphics systems...

You have successfully registered 1

Current available graphics systems

ASCIITree (ATree)

DAWNFILE (DAWNFILE)

G4HepRep (HepRepXML)

G4HepRepFile (HepRepFile)

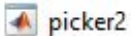
RayTracer (RayTracer)

VRML1FILE (VRML1FILE)

VRML2FILE (VRML2FILE)

gMocrenFile (gMocrenFile)

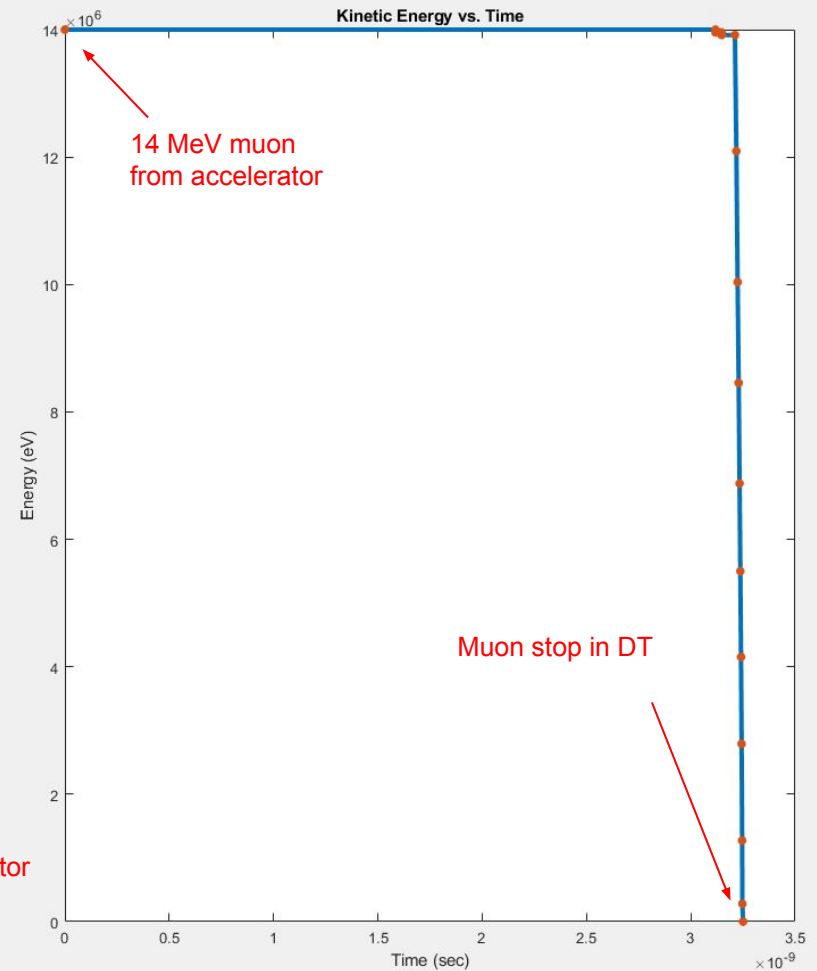
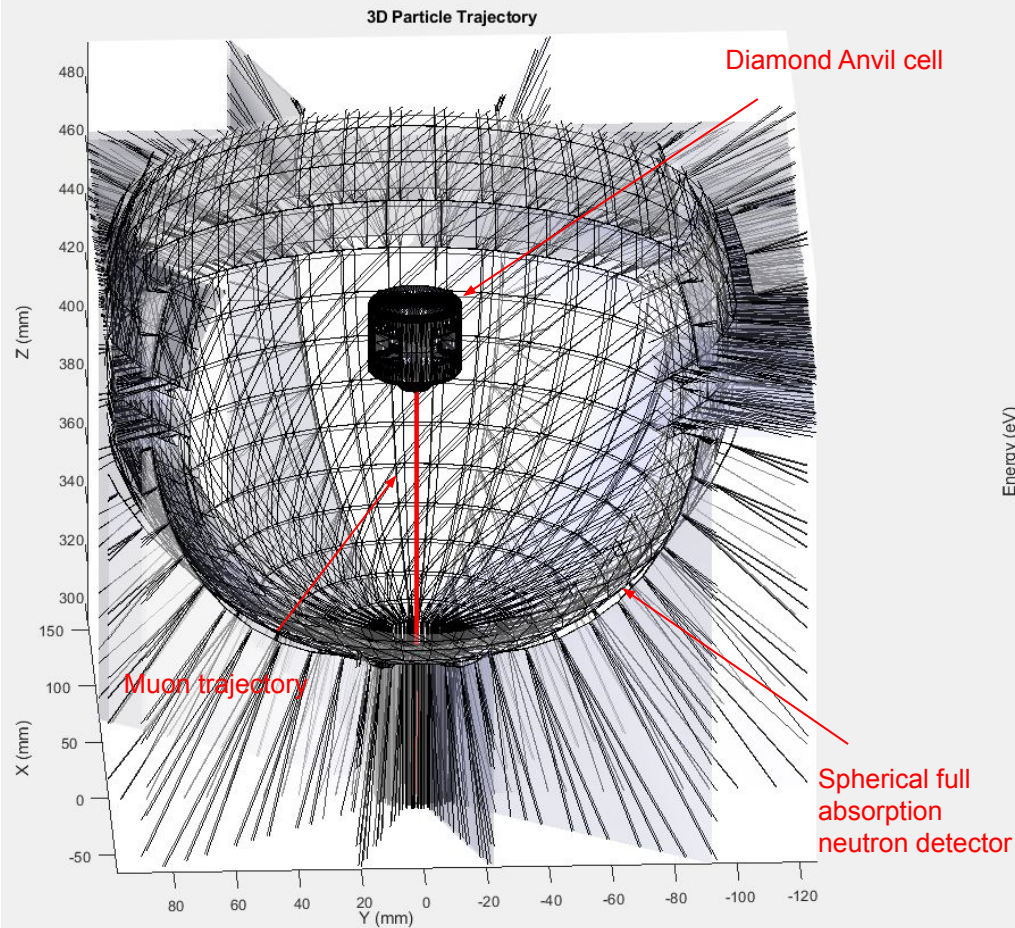
OpenGLImmediateQt (OpenGLQt, OGLI)



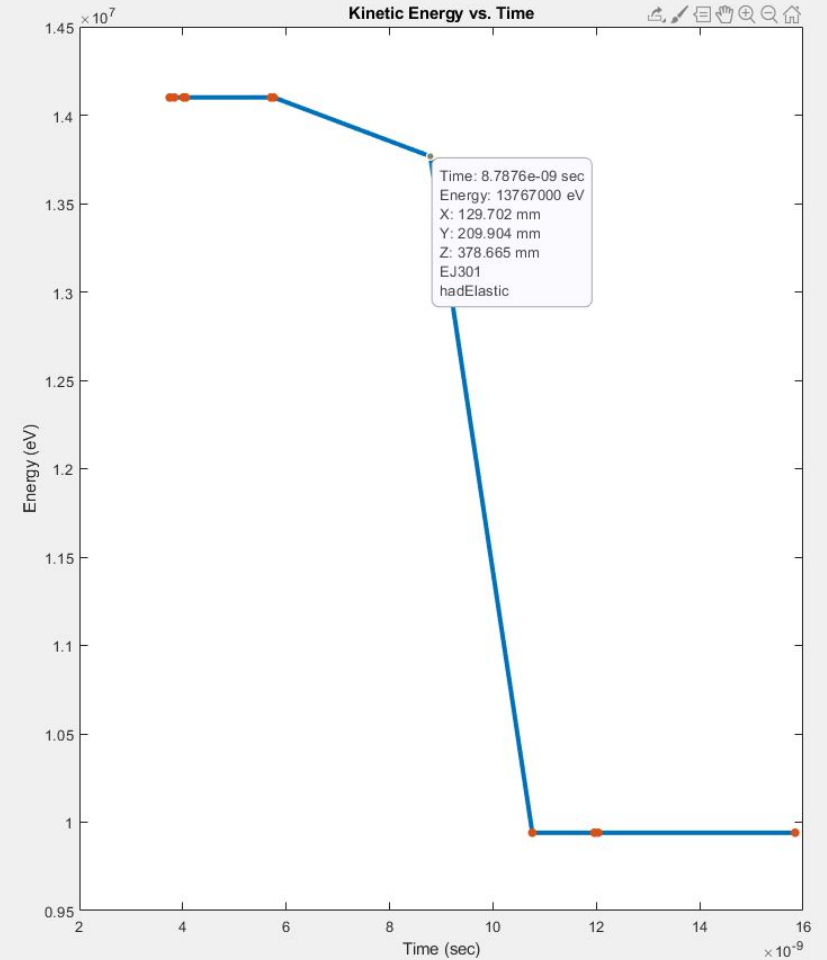
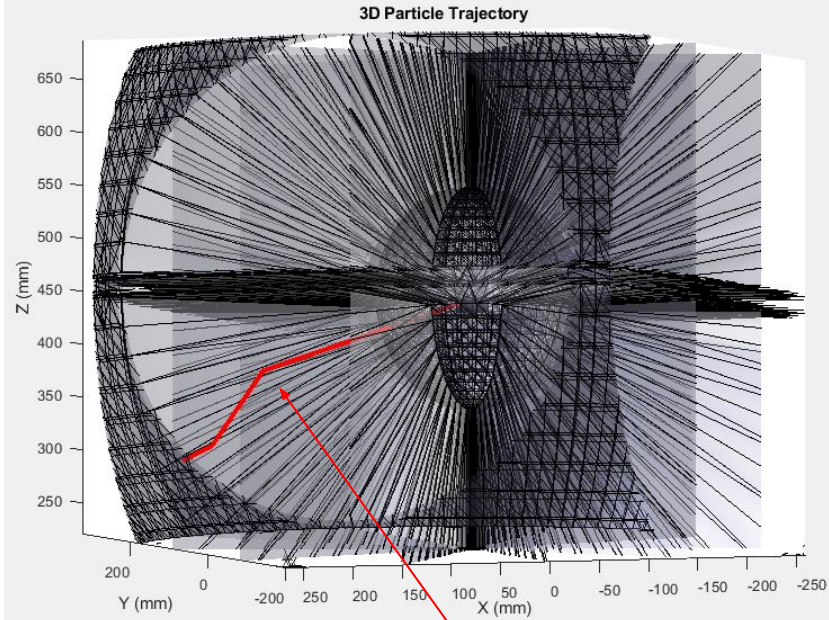
picker2

Job	Task	Fate	Event	Particle Track
job-2020-11-02-19-1	-	muonicAlphaStoppedInShell (0)	-	-
job-2020-11-02-22-0	task-1 ()	muonicAlphaStoppedInVacuum (0)	11	1<-0 mu-
job-2020-11-02-22-3		muonicAlphaStoppedInTorus (0)	15	1042<-1 e-
job-2020-11-02-22-5		muonicAlphaLeftVolume (0)	26	1043<-1 gamma
job-2020-11-02-22-5		muonicAlphaLeftVolumeAtCap (0)	90	1044<-1 gamma
job-2020-11-02-23-0		muonMinusCreated (490)		1045<-1 gamma
job-2020-11-09-23-2		muonMinusStoppedInFuel (0)		1046<-1 gamma
job-2020-11-09-23-2		muonMinusStoppedInShell (0)		1047<-1 MuH2
job-2020-11-10-00-0		muonMinusStoppedInVacuum (0)		1048<-1047 mu
job-2020-11-10-00-1		muonMinusStoppedInTorus (0)		1049<-1047 alp
job-2020-11-10-00-1		muonMinusDecay (0)		1050<-1047 neu
job-2020-11-10-08-4		muonMinusLeftVolume (0)		1051<-1050 C1:
job-2020-11-10-08-4		muonMinusLeftVolumeAtCap (0)		1052<-1050 pro
job-2020-11-10-08-4		alphaCreated (133)		16215<-1048 e-
job-2020-11-10-09-1		alphaStoppedInFuel (0)		16216<-1048 ga
job-2020-11-10-09-5		alphaStoppedInShell (0)		16217<-1048 ga
job-2020-11-10-14-2		alphaStoppedInVacuum (0)		16218<-1048 ga
job-2020-11-10-14-5		alphaStoppedInTorus (0)		16219<-1048 M
job-2020-11-10-15-1		alphaLeftVolume (0)		16220<-16219 r
job-2020-11-10-16-1		alphaLeftVolumeAtCap (0)		16221<-16219 z
job-2020-11-11-13-2		opticalPhotonCreated (238931)		16222<-16219 r
job-2020-11-11-14-0		muonicAtomDecay (127)		16223<-16222 C
job-2020-11-16-22-3		muonCatalyzedFusion (106)		16224<-16222 C

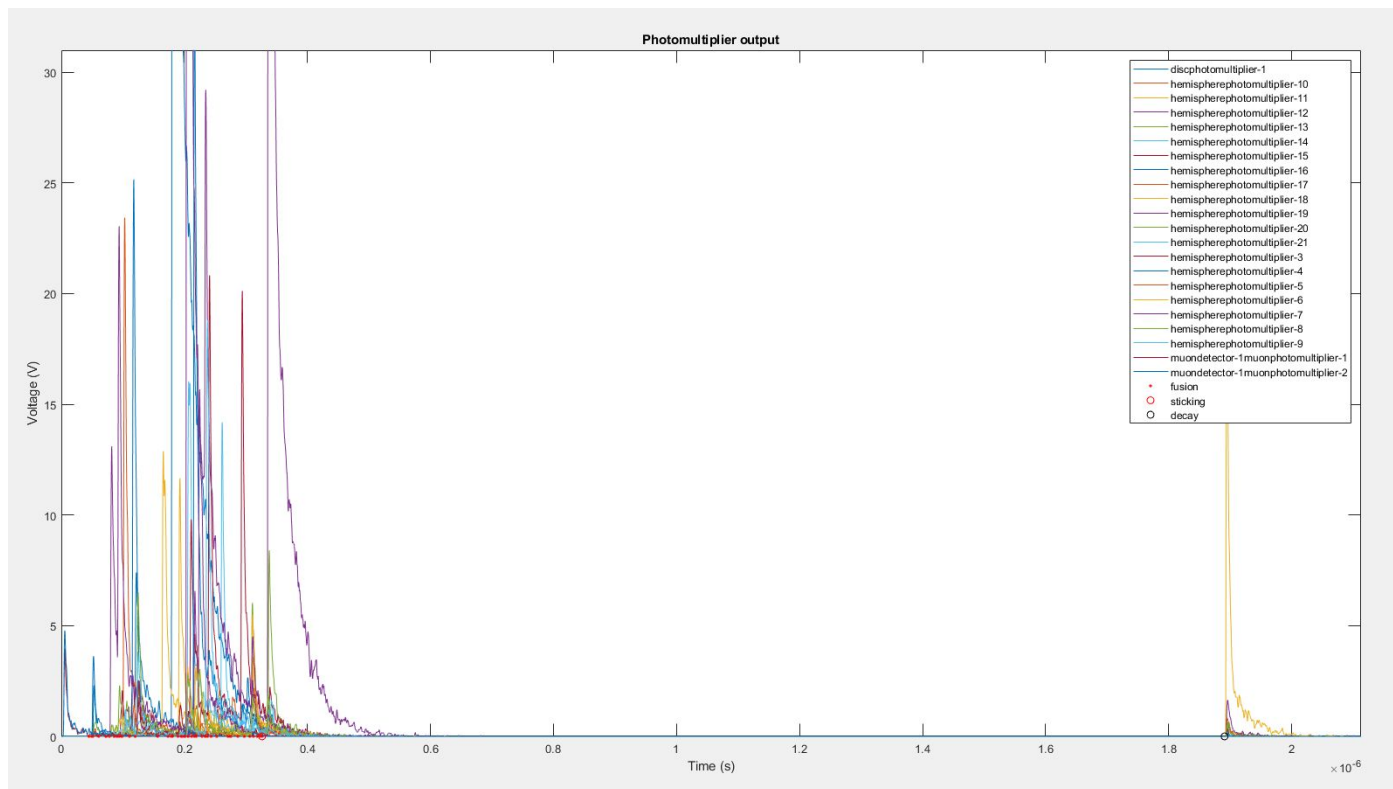
Muon stop in fuel



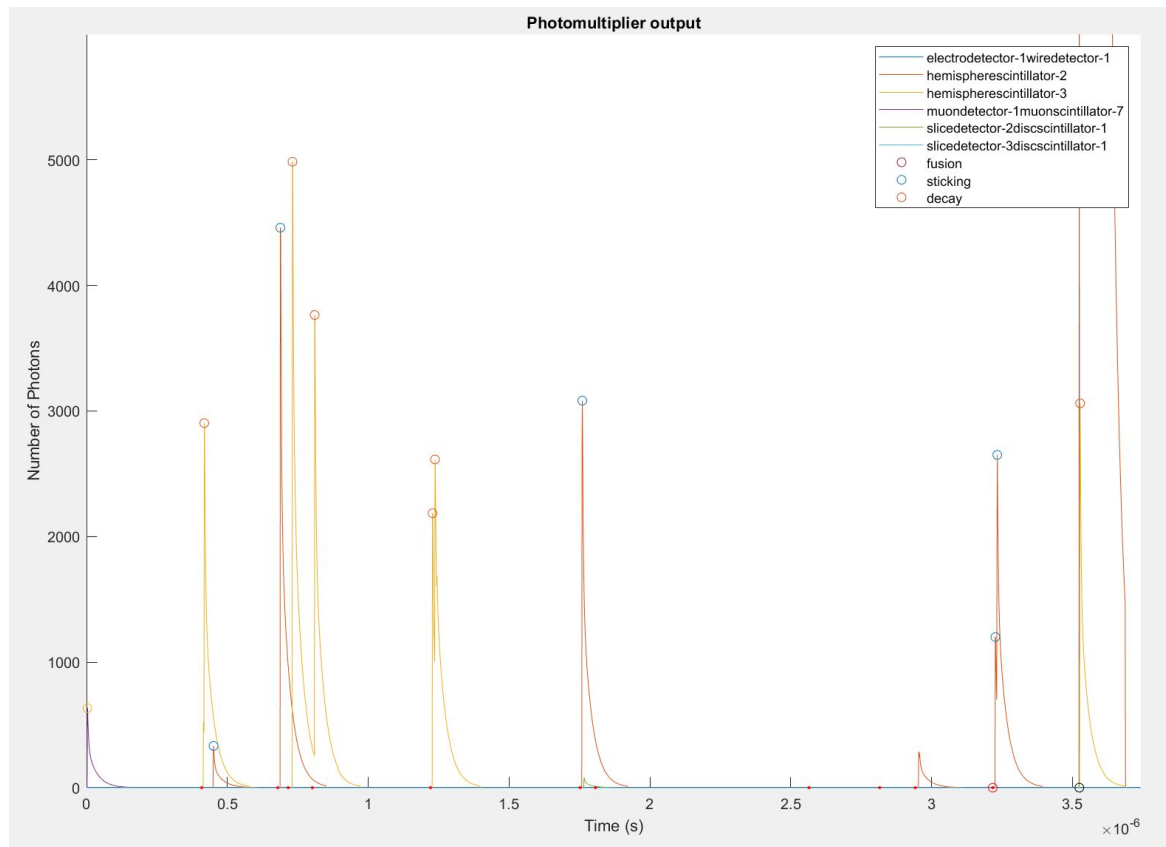
Elastic scattering of fusion neutron in detector volume



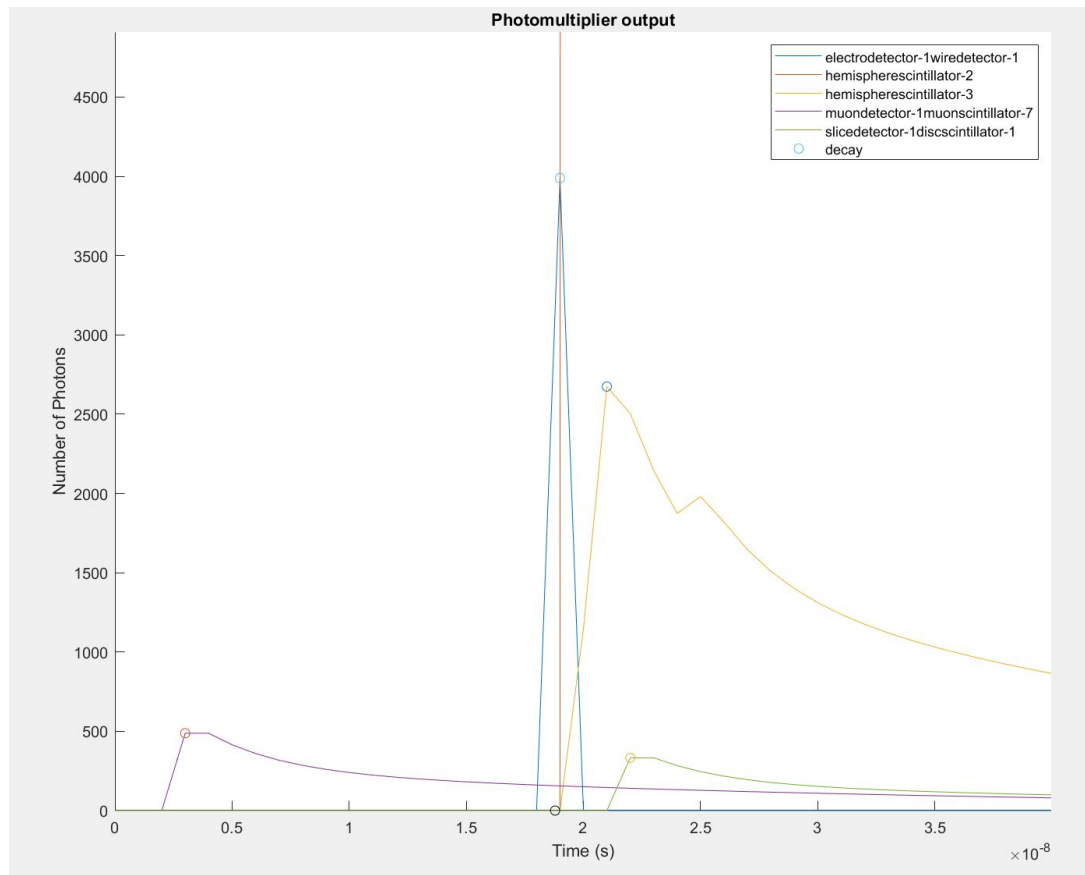
Typical DT fusion event (1 LHD, 300K)



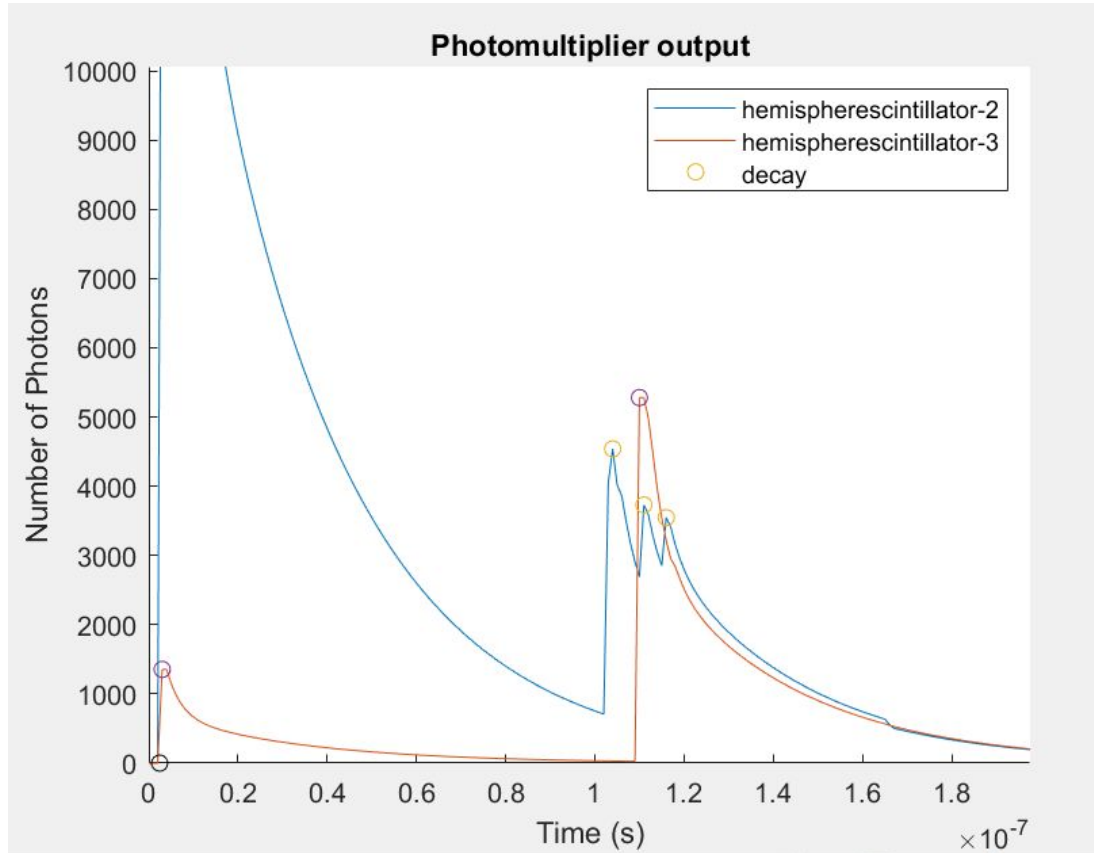
Typical DD fusion event (1 LHD, 300K)



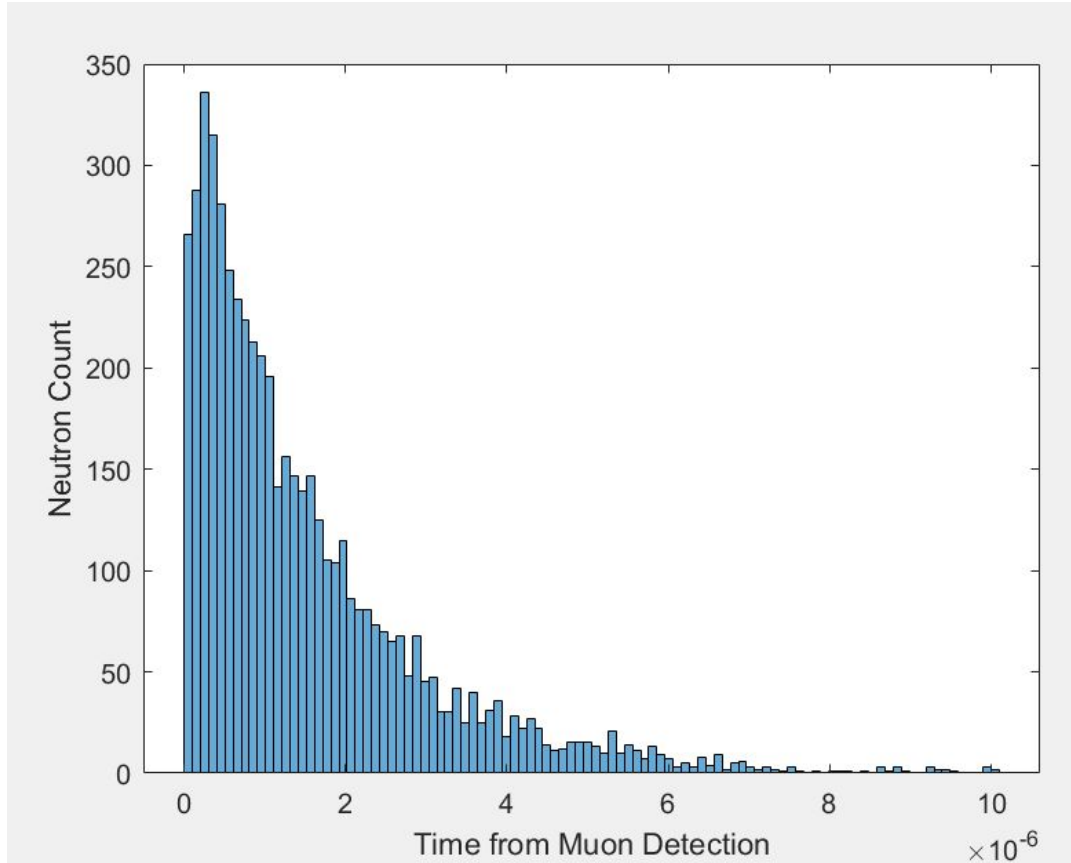
Typical non-selected event: μ - stop in diamond



Typical non-selected event: μ^- stop in collimator

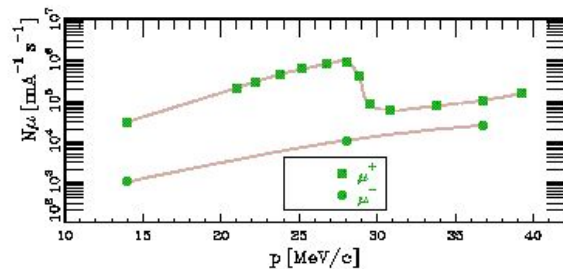


Neutron time spectra for GEANT4 simulation of 100,000 μ -

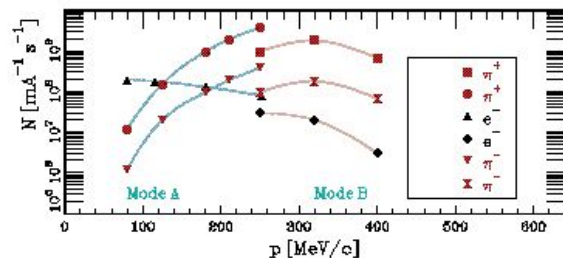


Corresponds to 2 minutes of real time; simulation time is similar.

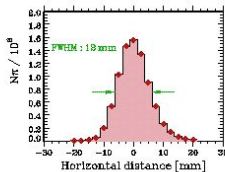
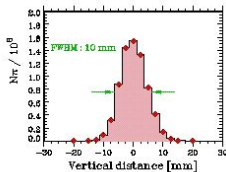
Rates and statistical uncertainty



- 4 minutes / cycling rate measurement
 - $\pm 1\%$ statistical uncertainty
 - 1,134 T/ φ conditions / 2 weeks



- 3 hours / sticking fraction measurement
 - $\pm 1\%$ statistical uncertainty
 - 60 T/ φ conditions / 2 weeks



(From PSI πE1 web page)



Sources of systematic uncertainty

- Mixture purity and condition
 - Palladium membrane purification
 - Mass spec at start and end
 - Real time raman
 - Chemical reaction with wall material
- Wall interaction
 - Both from geometry and from geometric uncertainty / misalignment
 - Can monitor frequency by decay electron time spectrum
- Spatial displacement by multiple reactivations per muon
- Multiple neutron scattering events inside detector
- (for cycling rate) Neutron detector calibration
- Pressure measurement (+/- 0.1 GPa)
- Temperature measurement (+/- 2 K)

Schedule

